UNIVERSIDADE DE LISBOA

FACULDADE DE MEDICINA LISBOA

TRABALHO FINAL
MESTRADO INTEGRADO EM MEDICINA

Instituto de Histologia e Biologia do Desenvolvimento

IDENTIFICATION OF KEY MOLECULAR PLAYERS IN THYMUS DEVELOPMENT

Leonor Magalhães

Orientado por:

Hélia Cristina de Oliveira Neves

MAIO'2022

ABSTRACT

The thymus is a conserved organ among vertebrates, derived from the endoderm of different pharyngeal pouches (PP), according to the species. In mammals, it derives from third PP (3PP) endoderm and in avian, from third/fourth PP (3/4PP) endoderm. Together with accessory thymi reports, this suggests a conserved potential to make a thymus in the different PP, independent of their specific anatomical location.

This thesis was included in a research project that aims to explore noncanonical pouches capacity to participate in thymus formation and the role of local mesenchyme of pharyngeal arches (PA) in regulating this thymic potential.

To start, heterospecific embryonic tissue associations *in vitro* and *in vivo* were performed, in stages prior to thymus formation. Then, I performed the histological analysis of the explants obtained. Our results showed, for the first time, the capacity of a noncanonical pouch (2PP) endoderm forming a thymus when associated with permissive mesenchyme. Additionally, we observed inhibitory properties in the dorsal (d) region of 2PA mesenchyme to the formation of the thymus, which confirmed regulatory properties of local mesenchyme.

To unravel the molecular signalling crosstalk during thymus formation, we mapped the transcriptomes of several isolated tissues: the 2PP and 3/4PP endoderm (thymic potential); and the 3/4PA and 2PAd mesenchyme (potential regulation). After initial bioinformatic analysis of the data, I performed further data analysis aiming to confirm gene identity and functional classification.

The transcriptomic analysis helped us to identify a common genetic program for thymic potential within the PP endoderm. Interestingly, the 3/4PP endoderm transcriptomic profile unveiled a previously undescribed Hox-code. We also identified the activation of distinct signalling pathways in different PA mesenchymal environments and in the context of specific endoderm-mesenchyme interactions.

Together, our results provided new data to the molecular signature involved in the initial specification of thymus primordium in the embryo.

Keywords: Thymic molecular signature; local mesenchymal modulators; high-throughput sequencing data.

RESUMO

O timo é um órgão linfático primário conservado apenas nos vertebrados. A sua origem embrionária provém da endoderme das várias bolsas faríngeas (BF) dependendo das espécies. Nos mamíferos, deriva da endoderme da terceira BF (3BF) e nas aves, da endoderme da terceira/quarta BF (3/4BF). Considerando ainda a existência de timos acessórios, tal sugere a existência de um potencial para formar timo conservado nas diferentes BF, independentemente de sua localização anatómica específica.

Esta tese inclui-se num projeto de investigação que procura explorar a capacidade de BF não-canónicas formarem timo e o papel do mesênquima local dos arcos faríngeos (AF) na regulação deste potencial tímico.

Inicialmente realizaram-se associações heteroespecíficas *in vitro* e *in vivo* de tecidos embrionários, em estadios prévios à formação do timo. De seguida, analisei a histologia dos explantes obtidos. Os resultados demostraram, pela primeira vez, a capacidade da endoderme de uma bolsa não-canónica (2BF) formar timo quando associada a mesênquimas permissivos. Adicionalmente, mostrou-se que a região dorsal (d) do mesênquima 2AF inibe o desenvolvimento tímico, demonstrando as propriedades reguladoras do mesênquima local.

Para descodificar a sinalização molecular ativada durante a organogénese do timo, mapeámos os perfis transcricionais de vários tecidos previamente isolados: a endoderme das 2BF e 3/4BF (com potencial tímico); e o mesênquima 3/4AF e 2AFd (regulador deste potencial). Após a análise bioinformática inicial do transcriptomas, investiguei mais detalhadamente os genes obtidos com o objetivo de validar a sua identidade e de os classificar funcionalmente.

A análise transcriptómica desvendou pistas para o programa genético conservado na endoderme das BF. Curiosamente, o perfil transcricional da endoderme 3/4BF revelou um código de genes Hox, não descrito anteriormente. Identificou-se, ainda, a ativação de distintas vias de sinalização, dependendo dos ambientes mesenquimais e de interações endoderme-mesênquima específicas.

Concluindo, estes resultados forneceram novas informações sobre a assinatura molecular da especificação inicial do primórdio tímico.

Palavras-chave: Assinatura Molecular do Timo; Moduladores do mesênquima local; Sequenciação de alto rendimento

TABLE OF CONTENTS

LIST OF FIGURES AND TABLES

FIGURES

TABLES

ACKNOWLEDGMENTS/AGRADECIMENTOS

Being a doctor has always been a dream for me, since little. However, I later discovered that besides the will to treat patients, understanding the how and why things happen amaze me just as much.

When I entered medicine, in the beginning of the 1st year, I felt overwhelmed by so many theoretical subjects, especially approaching concepts completely unknown to me. I fought hard to not just memorize them and actually, tried to understand the "whys". This feeling changed in the 2nd semester when I started studying Histology with the lecturer Hélia Neves, a Researcher. It may sound exaggerated, but I really enjoyed analysing all those "pink" images and hearing how brightly Hélia explored them. She taught us logic in the form of art, the art of recognizing a structure and understanding the reason for its existence and function. With time, questions and the growing desire to witness Science in the making arose. Hélia allowed me to enter the world of Research, thus changing the path of the remaining years of my course.

I will always be deeply grateful to Hélia, my supervisor of this Masters´ Final Work, for having welcomed me in this Project and for all the guidance and shared knowledge over these past 5 years. Hélia will always be a role model for me. Her way of thinking stuns me, making me grow as a medical student, an initiating researcher and a person. With her genius and modesty, she enthusiastically encouraged and taught me how to build rigorous and precise thought. Hélia also showed me that science is not made alone, instead it is based on sharing knowledge and discussion. Thank you for all your patience and care.

I would like to express my gratitude to Isabel Alcobia, who allowed me to accompany her in various lab procedures, and who has always supported this project with her characteristic peacefulness. Thanks to Margarida Gama-Carvalho and Domingos Henrique for the many dynamic and exciting discussions. I thank Margarida Gama-Carvalho for her essential contribution in bioinformatics analysis and for making a totally unknown world a little more perceptible. I would also like to thank Domingos Henrique for sharing his profound and extraordinary knowledge of genetics and much more, as well as his indispensable suggestions and contagious enthusiasm.

I would like to thank Edgar Gomes for having me at the Institute de Histologia e Biologia do Desenvolvimento. I also thank Leonor Parreira for the significant advice and comments. Thanks to Vitor Proa for guiding me through essential techniques for this project.

I would like to thank the Faculty of Medicine of the University of Lisbon and GAPIC for their “Education through Science” Program, encouraging the practice of scientific research during the Medical Course.

Last but not least, I want to thank my family for their unconditional support, for believing in me when sometimes I didn't believe in myself and for vibrating with me in the smallest victories. And, thanks to my mom, without her nothing would have been possible. To my friends, who through laughter and tears, pulled me back to reality and pushed me forward.

To all who contributed in some way to this work, my sincere thank you.

1

INTRODUCTION

THYMUS FUNCTION AND ARCHITECTURE

The thymus is a primary lymphoid organ, essential for T lymphocyte development and maturation. Only jawed vertebrates present this organ, which is one of the cornerstones of a functional adaptive immune system. During development, Lymphoid Progenitor Cells (LPC) migrate to the thymus, where they differentiate into T-cells and acquire the capacity to recognize and mount an immune response against foreign antigens (self-reactive) without being deleterious to the host tissues (self-tolerant) (Figueiredo et al., 2020; Hamazaki, 2015). This is called central immune tolerance. The inadequacy in developing a functional thymus can lead to immunodeficiency and/or autoimmunity (Rodewald, 2008).

In mammals, post-natal thymus is a bilobate organ located intrathoracically above the heart. The lobes are divided into lobules separated by mesenchymal septae, which continue as an enclosing capsule (Figure 1A). Each lobe is organized in two distinct histological regions exhibiting different microenvironments: cortical and medullary areas where final mature peripheral T cell repertoire is progressively selected (Anderson & Jenkinson, 2001; Nitta & Takayanagi, 2021; and Figure 1B).

Thymus consists in developing T cells (thymocytes) in intimate connection with the surrounding thymic stroma (Duah et al., 2021; Hamazaki, 2015). Thymic stroma is a unique microenvironment, mainly constituted by Thymic Epithelial Cells (TEC). Other stromal components are populations of hematopoietic cells, such as dendritic cells and macrophages; and mesenchymal cells, as endothelial cells and fibroblasts (Nitta & Takayanagi, 2021; Rodewald, 2008).

Thymus function is directly dependent on the complex architecture and variety of molecular microenvironments produced by TEC (Figure 1C). This epithelium exhibits unusual features, starting from its atypical three-dimensional meshwork shape that creates a scaffold while supporting the thymocytes migration (Ewijk et al., 1999). TEC also

releases crucial cues for thymocyte survival and proper differentiation and presents self-peptide/MHC complexes that guide lymphocytic selection (reviewed by Manley et al., 2011). TEC are divided according to morphology and functionality into cortical TEC, responsible for orchestrating the positive selection of immature T cells that recognize the self MHC; and medullar TEC, that enable the elimination of the autoreactive lymphocytes, preserving self-tolerant T cells (Klein et al., 2014; Rodewald, 2008; and Figure 1C).

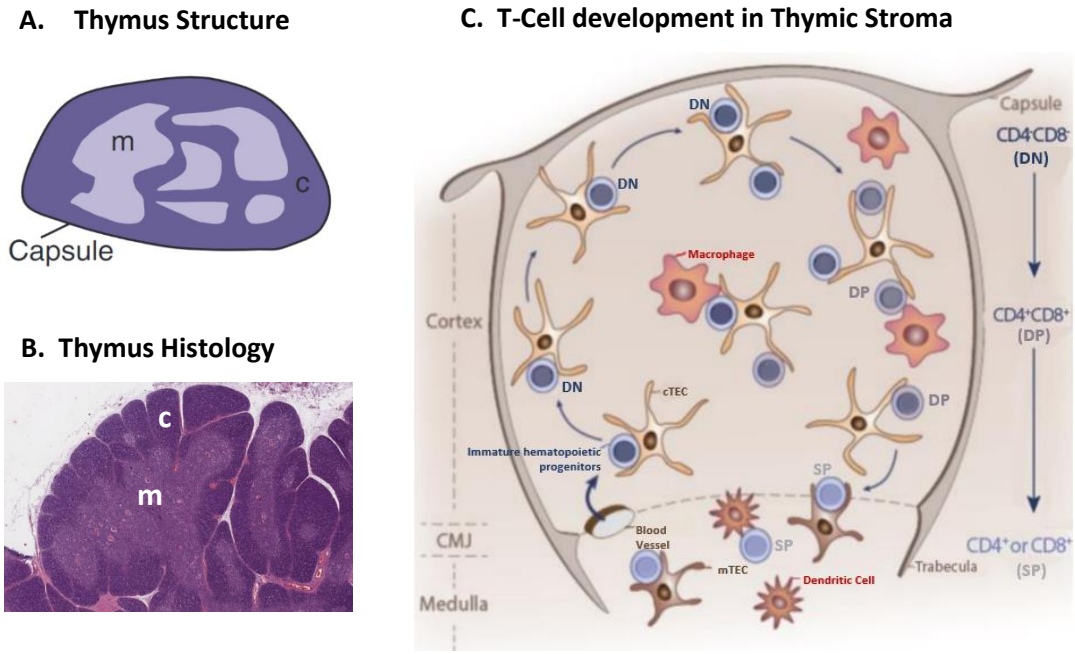

Figure 1. Structure and cellular components of Post-natal Thymus. A) Thymus presents a mesenchymal capsule, and it is divided into two histological regions: the cortex and the medulla. **B)** Histology of a neonatal thymus – microscope image of haematoxylin-eosin-stained section **C)** Schematic representation of T-cell development and interactions with thymus stromal cells, mainly TEC. Immature hematopoietic progenitors enter via CMJ blood vessels and migrate through the stroma, from cortex to medulla. During migration, thymocytes establish intimate contact with TEC, which promotes immature lymphocytes selection and maturation. In the cortex, thymocytes differentiate from $CD4^{-}CD8^{-}$ (DN) to $CD4^{+}CD8^{+}$ (DP). DP cells are then positively selected into either $CD4^{+}$ or $CD8^{+}$ (SP). Finally, in the medulla, self-reactive SP are negatively selected, the final stage of maturation to form the peripheric T-cell repertoire.
CMJ, corticomedullary junction; DN, Double Negative; DP, Double Positive; SP, Single Positive; TEC, Thymic Epithelial Cells. [Adapted from Figueiredo et al., 2020 and Gordon & Manley, 2011]

Vertebrate organism models such as mouse, chicken, and zebrafish have been crucial for studying thymus development, namely by providing morphological data and functional experimental approaches. In particular, later stages of thymus organogenesis, involving TEC and thymocyte maturation, have been extensively studied in the past decades. Although the mechanisms governing the earlier stages of thymus formation, involving endoderm-mesenchyme interactions, are still poorly understood, some important advances have been made.

EMBRYONIC ORIGIN OF THE THYMUS

Thymic Epithelium (TE) derives from the endoderm of the Pharyngeal Pouches (PP). During embryonic development, PP endoderm appear sequentially as bilateral structures outpocketing from lateral portion of the foregut (Rodewald, 2008; Vaidya et al., 2016; and Figure 2B).

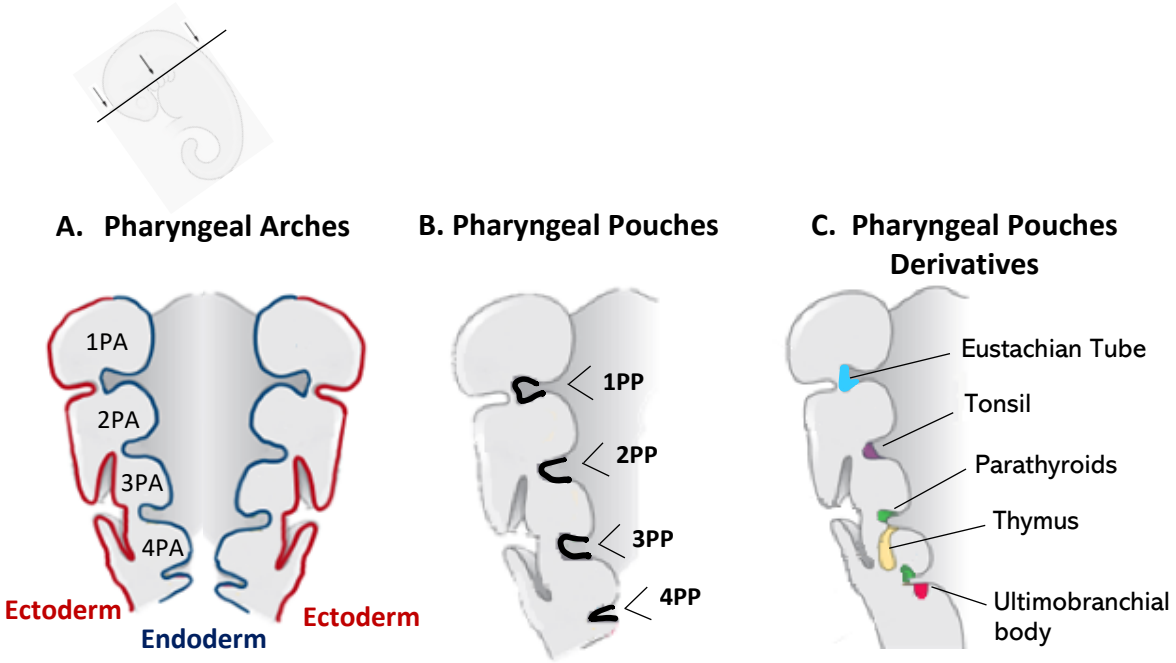

Figure 2. Schematic coronal section of the Pharyngeal Region. PAs are lined by an outer ectoderm layer and an inner endoderm layer. **B)** The endoderm evaginates towards ectoderm, forming the PP, that separates each PA. **C)** In human, the endoderm of the PP originates the Eustachian Tube (1PP), Tonsil (2PP), Parathyroid (3/4PP), Thymus (3PP), thyroid parafollicular cells - Ultimobranchial body (4PP). PA, Pharyngeal Arch; PP, Pharyngeal Pouch. [Adapted from Gilbert, S. F., & Barresi, M. J. F. (2016). Developmental biology (11th ed.)]

In 1975, Le Douarin and Jotereau proved for the first time the embryological origin of TE in the single endodermal germ layer of PP, using the chick-quail chimaera system (Le Douarin & Jotereau, 1975). The precise PP location of the thymus varies among different vertebrates (Figure 3).

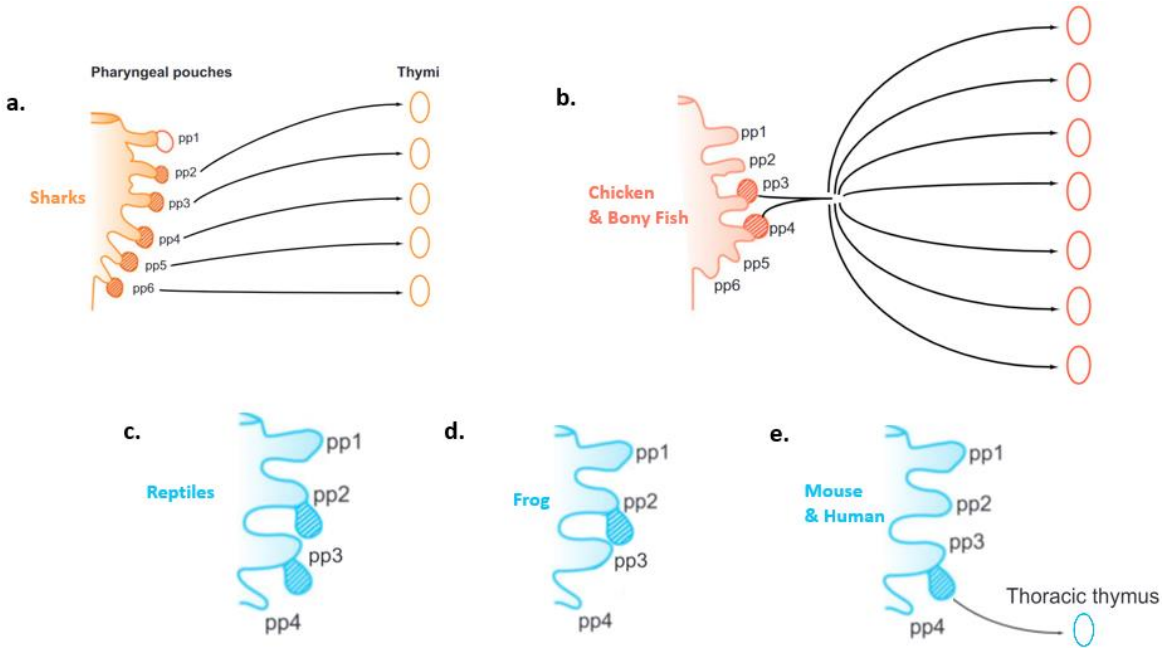

Figure 3. Phylogenetic comparison of thymus origin in jawed vertebrates. Vertebrate species present a flexible positioning of thymus rudiment along the pharyngeal pouches endoderm. Cartilaginous fish (Shark) is the most primitive vertebrate forming a thymus, which derives from the endoderm of 2PP to 6PP. In frogs, thymus rudiment derives from 2PP; in reptiles, from 2PP and 3PP; in mammals, birds and bony fish from 3PP and/or 4PP. PP, Pharyngeal Pouch [Adapted from Rodewald, 2008]

In chicken (and quail), TE derives from the 3/4PP endoderm, whereas in mammals it derives from the 3PP endoderm (Farley et al., 2013; Figure 2C). In addition, mesenchyme cells that surround the organ rudiment derive from the neural crest (NC) (K. Foster et al., 2008; Le Douarin & Jotereau, 1975).

Interestingly, despite the markedly distinct functions, TE shares the same embryologic origin to PT epithelium (common primordium rudiment) (Gordon et al., 2004; le Douarin & Jotereau, 1975; Neves, Dupin, Parreira, & le Douarin, 2012; and Figure 2C).

The major developmental stages of thymus formation are conserved among vertebrates (Rodewald, 2008). Thymus organogenesis initiates with the patterning of the pouches followed by rudiment specification (Figueiredo et al., 2016). Generally, thymus organogenesis can be divided into the following stages: 1) pouch positioning; 2) budding and outgrowth of thymus (and PT) rudiment; 3) detachment of primitive thymus from endodermal tube and 4) differentiation and migration of thymus towards its final position (Rodewald, 2008).

Epithelial-mesenchymal interactions are particularly important for early-stages of thymus organogenesis, the PP endoderm specification into thymus and parathyroid glands epithelia [between the aforementioned stages 1) and 2)] (Neves, Dupin, Parreira, & Le Douarin, 2012). Hereafter, TEC and lymphocytes interact synergistically promoting mutual growth and maturation, known to as "thymic crosstalk" at late-stages of thymus organogenesis (Bleul et al., 2006).

Thymus Development In Mouse

Thymus organogenesis is better detailed in the mouse model. On mouse (m) Embryonic (E) day 9.5 (mE9.5), the 3PP endoderm starts to proliferate to form bilateral primordia, initially as a single cell layer of columnar epithelium continuous to the pharynx (Gordon et al., 2004). At the same time, this epithelium (future T/PT common primordium) is surrounded by NC-cells that promote its development and, later-on, will form the thymus capsule (reviewed by Figueiredo et al., 2020 and Gordon & Manley, 2011). From mE10.5-E11.5, pouches develop into a multi-layered pseudostratified epithelial structure, with a central lumen (Figure 4A).

On mE11.5 in mice, T/PT primordium is patterned into ventral thymus´s domain and dorsal PT´s domain (Gordon et al., 2004; Gordon & Manley, 2011; Manley et al., 2011). Simultaneously, LPC colonize the thymus rudiment and the later starts to detach from the pharynx, guided by NC cells that promote endodermal apoptosis (Bleul et al., 2006; reviewed by Figueiredo et al., 2020 and Gordon & Manley, 2011; and Figure 4B).

Around mE12.5 signals from NC cells and cellular intercalation promote thymus and PT rudiments separation, directing thymus migration (Figure 4C). In mice, the developing

thymus has two successive waves of LPC colonization. The first wave occurs around mE11.5 and the second one at mE15, which leads to final thymic maturation (Nowell et al., 2007; Ramond et al., 2014).

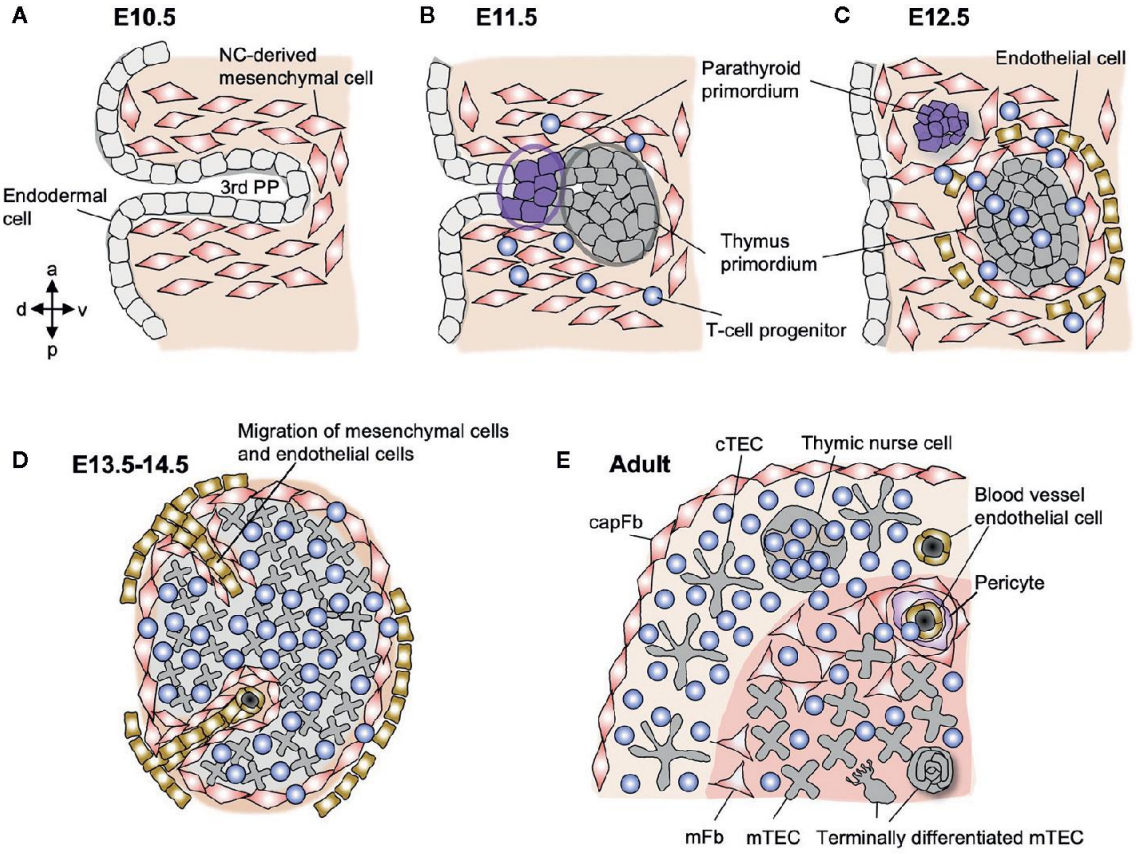

Figure 4. Embryonic and adult stages of thymus development in mice. A) In E9.5-10.5, a single layer of 3PP endoderm proliferates surrounded by NC-derived mesenchymal cells. **B)** Around E11.5, the T/PT primordium is formed and patterned into the thymus domain and parathyroid gland domain. At the same time, lymphoid progenitors start to colonize the thymic rudiment. **C)** On E12.5, NC-derived cells promote thymus and parathyroid rudiments separation. **D)** A fraction of mesenchyme cells migrates into the epithelial rudiment, as the other part remains in the periphery to form the future thymic capsule. **E)** In the adult, thymus is enclosed with a capsule. Thymic stroma has a highly organized configuration that promotes T-cell development, through TEC and mesenchymal cells maintain close functional and spatial interactions. TEC and mesenchymal cells interact functionally and spatially. A, Anterior; D, Dorsal; capFb, Capsular Fibroblast; E, Embryonic day; mFb, Medullar Fibroblast; mTEC, Medullar Thymic Epithelia Cell; NC, Neural Crest; PP, Pharyngeal Pouch; P, Posterior; V, Ventral. [Adapted from Nitta & Takayanagi, 2021]

THYMUS DEVELOPMENT IN CHICKEN

In avian embryos, thymus and parathyroids epithelia derive from the 3/4PP endoderm. TE detach from the pharynx as a cord of epithelial cells, at chicken (c) embryonic day 5 (cE5) [Hamburger and Hamilton-stage 26, HH26 (Hamburger & Hamilton, 1992)] (Neves, Dupin, Parreira, & le Douarin, 2012). NC cells surround the endodermal primordium forming a mesenchymal capsule and, at c6.5 (HH-stage 29), LPC start colonizing the TE (Neves, Dupin, Parreira, & le Douarin, 2012). In chicken, TE colonization by LPC occurs in three waves: the first wave at cE6.5, before thymic rudiment vascularization, and the other two at cE12 and cE18 (reviewed by Garcia et al., 2021).

All the described events rely on a crosstalk of several signalling pathways and transcription factors (reviewed by Abramson & Anderson, 2017), detailed in the following section.

MOLECULAR REGULATORS OF THYMIC EPITHELIUM COMMITMENT

Recently, major efforts have been made to unveil the molecular signals involved in pharyngeal endoderm specification into thymus fate.

The thymic rudiment specification is dependent on the transcription factor Fork-head Box N1 (Foxn1). Foxn1 was identified as the first marker of TE (Nehls et al., 1994), known to be essential for its proliferation and differentiation (Blackburn et al., 1996; Nehls et al., 1996). Foxn1 starts to be expressed at mE11.25 in the thymic rudiment.

Foxn1-deficiency mutant mice (*Nude*) were described as having congenital athymia while exhibiting severe immunodeficiency (Flanagan, 1966). Although mutant mice lack a functional thymus, a thymic primordium is formed and reaches the final adult thymus location (Nehls et al., 1994; Nehls et al., 1996). Since there is no TE colonization by LPC, the thymus rudiment fails to properly differentiate into TEC and degenerates into cysts (Vroegindeweij et al., 2010; reviewed by Vaidya et al., 2016).

PT rudiment specification and differentiation is known to lean on the expression of parathyroid specific marker, glial cells missing homolog 2 (Gcm2) (Liu et al., 2007). Gcm2 starts to be expressed in the 3PP at E9.5 (Figure 5A) and at E10.5 it defines the T/PT

common primordium (Gordon et al., 2001; and Figure 5B). During T/PT primordium patterning (at E11-E11.5, as described above), Foxn1 and Gcm2 occupy complementary domains of 3PP endoderm, ventral and dorsal regions, respectively (Gordon et al., 2001; and Figure 5C).

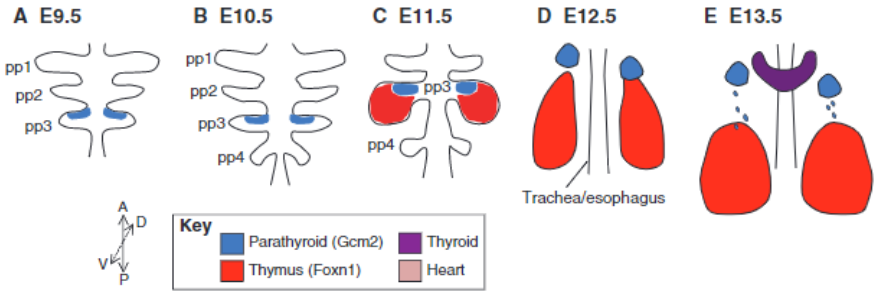

Figure 5. Schematic representation of the sequential thymic and PT markers expression domains in PP and respective rudiments (in mice). A) Around E9.5, Gcm2 starts to be expressed in the 3PP endoderm. **B)** At E10.5, the 4PP is formed. **C)** In 3PP, at E11.5, the common primordium patterns into two domains, ventral domain (thymus rudiment) and dorsal domain (parathyroid rudiment). These domains express Foxn1 and Gcm2, respectively. **D)** By E12.5, the organ rudiments that have detached from the pharynx, separate from each other. **E)** At E13.5, the rudiments migrate to their final positions. A, Anterior; D, Dorsal; E, Embryonic day; PP, Pharyngeal Pouch; P, Posterior; V, Ventral. [From Gordon & Manley, 2011]

In chicken embryos, the organ rudiments are inverted and consequently Foxn1 is expressed on the dorsal domain of both 3/4PP endoderm at cE4.5 (HH-stage25). Conversely, Gcm2 locates in the ventral domain of the 3/4PP endoderm, at cE3.5 (HH-stage 22) (Neves, Dupin, Parreira, & le Douarin, 2012). The early expression pattern of Gcm2 prior to T/PT common primordium formation may represent the evolutionary legacy or may suggest the need to preserve the PT fate in the PP endoderm (Figueiredo et al., 2020).

Even though Foxn1 and Gcm2 are the first recognized markers of thymus and PT differentiation, respectively, upstream factors directly involved in lineage commitment of these organs are largely unknown.

Some transcription factors known to act upstream of Foxn1 and Gcm2 are Tbx1 and the Hox-Eya-Six-Pax network (Hoxa3, Eya1, Six1, Pax1, Pax9), whose abnormalities lead to impaired thymus organogenesis (Vaidya HJ et al., 2016; and Figure 6).

Tbx1 is a transcription factor expressed in both PP endoderm and mesodermal core of Pharyngeal Arch (PA), since mE8.0 (Jerome & Papaioannou, 2001; Figure 6). Tbx1 mutations are responsible for DiGeorge syndrome in humans, which displays agenesis of 2-4PP and concomitant malformation of PP-derivate organs (Vitelli et al., 2002). Consequently, this syndrome presents cardiovascular defects, abnormal facial features, aplasia or hypoplasia of the thymus and PT glands (Jerome & Papaioannou, 2001). This gene plays a significant role in PA segmentation and PP formation, by interacting with several signalling pathways through various effectors, such as Fgf8 and Foxi3 (reviewed by Figueiredo et al., 2020; and Figure 6).

The Hox-Eya-Six-Pax network genes are involved in early 3PP endoderm patterning and T/PT primordium development, as null mutants for each gene have normal pouch formation but hypoplastic organs (reviewed by Figueiredo et al., 2020; and Figure 6).

Hoxa3 belongs to the homebox family of transcription factors and is expressed in 3/4PP endoderm and adjacent NC cells from E8.5-E9.5, in mice (Gordon, 2018) . Hoxa3 null phenotype shares similarities with DiGeorge Syndrome phenotype (Ivins et al., 2005). Although normal 3/4PP is formed and both Foxn1 and Gcm2 initiate their expression, the primordium undergoes apoptosis (Chojnowski et al., 2014). Hoxa3 is placed upstream in the network cascade, above Eya1/Six1 and Pax1/Pax9 (reviewed by Figueiredo et al., 2020; Figure 6).

Eya1 is a transcription co-activator, expressed from mE9.5 in the pharyngeal endoderm, NC-derived mesenchyme and ectoderm (Xu et al., 2002; review in Figueiredo et al., 2020). Eya1 mutant lack thymus and PT gland, with absence expression of Foxn1 and Gcm2 (Xu et al., 2002). Six1 is a transcription factor, whose expression is Eya1-dependent (X. Li et al., 2003; Xu et al., 2002; review in Figueiredo et al., 2020). Six1 mutant phenotype is similar to Hoxa3 null mutants (Zou et al., 2006).

The transcription factors Pax1 and Pax9 have their expression restricted to the pharyngeal endoderm at mE8. Their expression is maintained during further development of TEC (review in Figueiredo et al., 2020; and Figure 6). $Pax1^{-/-}$ mutant presents hypoplastic thymic and PT glands; in $Pax9^{-/-}$ mutant, the T/PT primordium does not detach from the pharynx, developing into a polyp-like structure (Hetzer-Egger et al., 2002; Su et al., 2001). Despite being colonized by LPC, this structure is filled with apoptotic cells

(reviewed by Figueiredo et al., 2020). Gata3 is initially expressed in T/PT primordium, becoming restricted to the Gcm2 domain later, when the Foxn1 domain is also established (Figueiredo et al., 2016; reviewed by Figueiredo et al., 2020; and Figure 6).

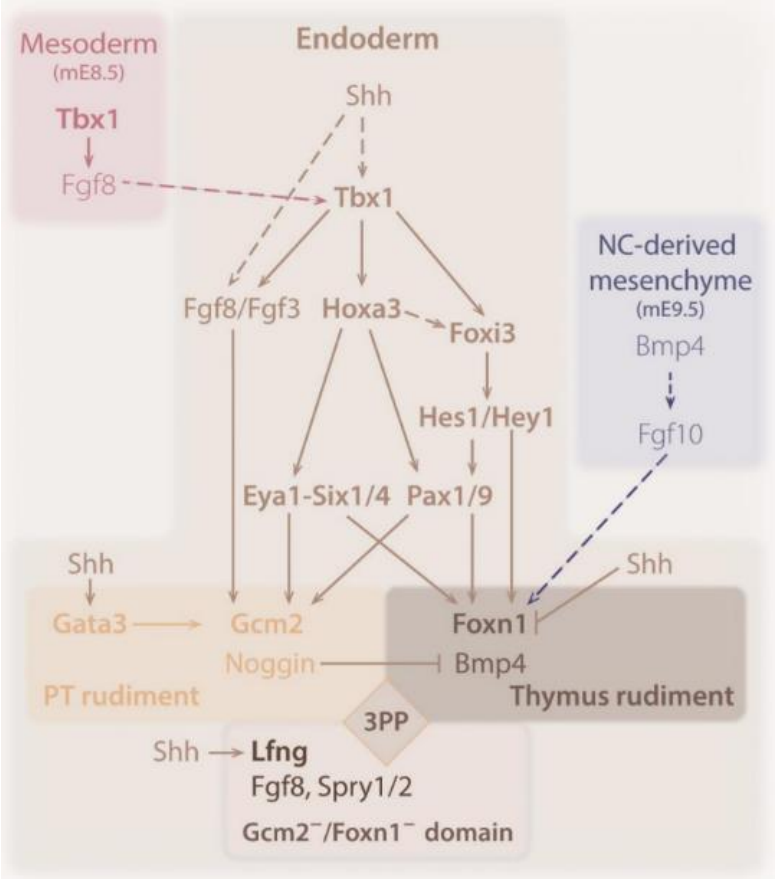

Figure 6. Schematic diagram of factors potential interactions in the early steps of the thymus development. Tbx1 and Hox-Eya-Six-Pax regulatory network of transcription factors operate during early initiation of T/PT primordium formation and act upstream Foxn1 and Gcm2.
Color code of the different tissue compartments: Endoderm—from yellow to dark brown; mesoderm—rose; NC mesenchyme—blue. Solid and dashed lines indicate known and hypothetical interactions, respectively. Bold font—transcription factor. Regular font—signalling molecule. E, Embryonic day; m, Mice; NC, Neural Crest [From Figueiredo et al., 2020]

In addition to the transcriptional factors portrayed, major signalling pathways like bone morphogenetic protein (BMP), fibroblast growth factor (FGF), Wingless-int (Wnt), Notch, and Hedgehog, were also shown to be involved in the 3/4PP patterning and the early phases of thymus organogenesis (reviewed by Figueiredo M et al., 2020; and Figure 6).

During the past years, H. Neves and collaborators at the Instituto de Histologia e Biologia do Desenvolvimento (IHBD)-FMUL took advantage of the chicken model and chick-quail chimaera system to study epithelial-mesenchyme interactions at early stages of thymus organogenesis. This line of research shown the importance of Notch signalling for TE specification and parathyroid epithelium differentiation, in a Hedgehog dependent manner (Figueiredo et al., 2016). In addition, Foxn1 expression was unexpectedly detected in the 2PP endoderm (not a canonical pouch for thymus formation in avian), and its expression was modulated by Hedgehog signalling, in a similar manner to 3/4PP (canonical pouch for thymus formation in avian) (Figueiredo et al., 2016).

These findings suggest that Foxn1-expression domains in the distinct endodermal pouches may embody a conserved potential to develop a thymus. In agreement, thymus derives from different pouches among jawed vertebrates (Rodewald, 2008), as well as the number of thymus organs per animal and the final anatomical positions of thymic lobes. Furthermore, accessory thymi were found in the cervical region in humans (Norris, 1938; Van Dyke, 1941) and mice (Dooley et al., 2006; Terszowski, 2006).

As 2nd year medical student (2017/2018), my passion for Histology and interest for research inspired by H. Neves classes, headed me to the IHBD. When I arrived, H. Neves and her colleagues were just starting to seek this hypothesis. My work in the project started the year after, with the first application for the 22nd Program “Education for Science” (2018/2019).

2
OBJECTIVES

Considering the known diversity of PP location of thymic rudiment among vertebrates along with the previous findings of our Lab (Foxn1 expression in non-canonical pouches), we hypothesised the existence of a phylogenetically conserved genetic program to "make a thymus" embodied in the endoderm of different PP, independent of their specific anatomical location. In addition, this program may be (or not) restricted by differential, yet unknown, molecular cues provided by the adjacent pharyngeal arch (PA) mesenchyme.

This thesis was included in a project of our research team aiming to investigate:
1) if the potential to “make a thymus” is conserved in the endoderm of all pharyngeal pouches; if so, to unveil the conserved genetic program to “make a thymus” and
2) if the mesenchyme of the pharyngeal arches regulates thymus formation; if so, to identify the signals responsible for this regulation.

To achieve these objectives, we used the modified chick-quail chimaera system (Figueiredo et al., 2016; Figueiredo & Neves, 2018, 2019), in a stage of development prior to Foxn1 expression. Heterospecific associations of isolated embryonic tissues from quail PP endoderm (2PP and 3/4PP) and chicken mesenchyme (from several locations) were performed to evaluate the capacity to form a functional thymus. After *in vitro* and *in ovo* development, explants derived from the associated-tissues were collected and analysed by conventional histology and immunochemistry.

During the first part of the project, I have participated in the preceding steps of the functional assays (in particular, eggs preparation for tissue isolation) and actively followed the running *in vitro* and *in ovo* experiments. My major contribution was performing all histological analysis. Briefly, all serial sections of the heterospecific associations samples (around 50) were qualitatively and quantitatively examined. I’ve learned to identify all growing embryonic tissues in the samples and, in particular, the thymus and PT glands.

Afterwards, we proceed to the transcriptomic analysis of isolated embryonic tissues by RNA sequencing, to find the genetic program to “make a thymus” and its regulatory signals.

In this part of the project, I attended to the multiple meetings and contributed to the discussions of the results obtained after bioinformatic analysis. I’ve learned with our bioinformatic expert how these data are obtained and analysed. My major participation was to confirm gene identity and functional classification of the final set of genes obtained in the different tissues (total of ~2100 genes). For this analysis, I employed several bioinformatic platforms such as Ensembl, GEISHA (Gallus Expression In Situ Hybridization Analysis), MGI (Mouse Genome Informatics), UniProtKB, g:Profiler, Enrichr and inBio Discover.

3

MATERIALS AND METHODS

This section is a modified version of the correspondent one found in:
Isabel Alcobia, Margarida Gama-Carvalho, Leonor Magalhães, Vitor Proa, Domingos Henrique, Hélia Neves (2022). *Thymus formation in uncharted embryonic territories.* Available in BioRxiv doi:10.1101/2022.03.09.483697 https://biorxiv.org/cgi/content/short/2022.03.09.483697v1

FUNCTIONAL ASSAYS

Isolation of quail and chick embryonic tissues

Fertilised Japanese quail (*Coturnix coturnix japonica*) and chicken (*Gallus gallus*) eggs were incubated at 38 °C in a humidified incubator and embryos were dissected at specific times of development. Embryos were staged by microscopic examination according to Hamburger and Hamilton stages (HH, Hamburger and Hamilton, 1951) in the chick and to corresponding HH-stages in the quail. Isolation of 1PP, 2PP and 3/4PP endoderm was performed at embryonic day 3 (E3, HH-stage 21) of quail embryos and at E2.5 (HH-stage 19-20) of chick embryos, as previously described (Figueiredo & Neves, 2019; Le Douarin & Jotereau, 1975; Neves, Dupin, Parreira, & Le Douarin, 2012) (Figure 7). Briefly, pharyngeal tissues were obtained by treating the wall of the embryonic pharynx with a solution of pancreatin (8 mg/ml, Sigma) for 30–90 min on ice, which allowed separation of pure endoderm from the pharyngeal mesenchyme. Mesenchymal tissues of E2.5–E3 (HH-stages 18–19) chick embryos were dissociated from endodermal and ectodermal tissues by enzymatic digestion with pancreatin using the same procedure described above. Somatopleura tissues were obtained from the embryonic territories at the level of somites 19–24 (Figueiredo & Neves, 2019).

In vitro tissue culture assay

1PP, 2PP and 3/4PP endoderm were isolated from E3 quail embryos and grown in association with mesenchymal tissues isolated from E2.5 chick embryos, as described (Figueiredo & Neves, 2019; Neves, Dupin, Parreira, & Le Douarin, 2012; and Figure 7). Different sources of mesenchymal tissues were isolated: Somatopleura mesoderm; 3/4PA mesenchyme; 2PA mesenchyme; ventral territory of 2PA mesenchyme (2PAv); dorsal

territory of 2PA mesenchyme (2PAd); 1PA mesenchyme. In brief, 2–3 endodermal explants (1PP, 2PP or 3/4PP endoderm) were combined with 2–3 mesenchymal explants on Nucleopore membrane filters (Millipore) supported by fine meshed metal grids (Goodfellows). The grids were then placed into culture dishes and partly immersed in RPMI-1640 (Sigma) supplemented with 10% FBS (Invitrogen) and 1X Pen/Strep (Invitrogen). The heterospecific associated tissues were cultured for 48 h at 37 °C in a humidified incubator containing 5% CO_2. Following the incubation period, cultured tissues were either used for RNA isolation or grafted on the chorioallantoic membrane (CAM) of E8-chick embryos (Figure 7). Grafted tissues were allowed to further develop in ovo for 10 days in a humidified incubator at 38 °C, as described (Le Douarin & Jotereau, 1975; Neves, Dupin, Parreira, & Le Douarin, 2012; and Figure 7).

Immunohistochemistry

CAM-derived explants were fixed overnight in 4% paraformaldehyde/PBS at 4°C. Samples were then processed for immunohistochemistry, as described (Figueiredo et al., 201; and Figure 7). Paraffin sections of explants developed *in ovo* for 10 days were analysed by haematoxylin-eosin staining (H&E) to determine the number, size and morphology of thymic lobes and parathyroid glands formed. Sections of CAM-explants were further treated for immunocytochemistry with the mAb Quail PeriNuclear (QCPN) antibody (for labelling of quail cells), CD3 antibody (Dako M725429-2, for labelling T-lymphoid cells) and anti-pan [Lu-5] Cytokeratin antibody (Pan CK) (Abcam; for labelling epithelial cells), as described (Figueiredo & Neves, 2018; Neves, Dupin, Parreira, & Le Douarin, 2012) .

Microscopy

H&E and immunohistochemistry images were collected using Software Leica Firewire and Leica DM2500 microscope with Leica DFC420 camera.

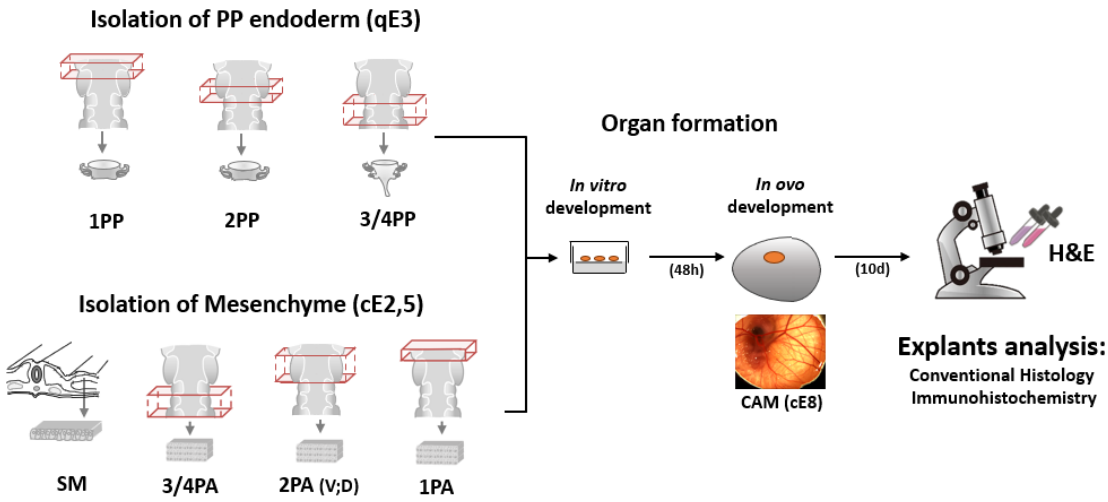

Figure 7. Schematic representation of the functional assays, using modified chick-quail chimera system. Isolation of endodermal tissue from a quail (E3) and mesenchyme tissues from chicken (E2.5) was performed. Several combinations of endoderm and mesenchyme tissues were *in vitro* associated for 48h. The heterospecific cultured tissues were then grafted into the CAM of a chicken embryo (E8) and allowed to develop *in ovo* for further 10 days. The explants were then collected and analysed by conventional histology and immunochemistry. c, Chicken; CAM, Chorioallantoic Membrane; D, Dorsal Territory; E, Embryonic day; H&E, Haematoxylin-Eosin stain; PA, Pharyngeal Arch; PP, Pharyngeal Pouch; q, Quail; SM, Somatopleura Mesoderm; V, Ventral Territory.

TRANSCRIPTOMIC PROFILE ACQUISITION AND ANALYSIS

This part of the project was done in collaboration with, Margarida Carvalho, at FCUL, who performed the bioinformatic analysis.

RNA library preparation

Total RNA from the samples was extracted using a combination of TRIzol reagent (Invitrogen) and RNeasy Mini Kit (QIAGEN) according to the manufacturer's instructions (Figueiredo et al., 2016). RNA samples were obtained from freshly isolated embryonic tissues of quail endoderm at E3 and chicken mesenchyme at E2.5. The isolated endoderm tissues were 2PP endoderm, 3/4PP endoderm and central pharynx region (Pharynx). The isolated mesenchyme tissues were 3/4PA mesenchyme and dorsal territory of 2PA mesenchyme (2PAd). Three replicates of 15-20 explants per sample were generated for each condition. Total RNA samples were validated for concentration and integrity (RIN ≥ 7) and 1 µg of total RNA was used to prepare libraries with the

Stranded mRNA Library Preparation Kit according to manufacturer's instructions. Libraries were sequenced on an Illumina Novaseq platform with paired end 150bp reads (acquired as a service to STAB Vida), with an average yield of 25M reads per sample (R1+R2). The raw RNA-Seq datasets are available through the European Nucleotide Archive under the study accession number PRJEB51508 (*Gallus gallus* dataset) and PRJEB51507 (C. coturnix dataset).

RNA-Seq data analysis

Following quality assessment using FastQC version 0.11.5 (https://www.bioinformatics.babraham.ac.uk/projects/fastqc/), Cutadapt was used to remove sequencing adaptors and trim the first 10 nucleotides (Martin, 2011). The trimmed data was then filtered using in-house developed Perl script in order to remove reads with unknown nucleotides, homopolymers with length ≥50 nt or an average Phred score <30 (Amaral et al., 2014). Remaining reads, corresponding on average to 80% of the raw data, were aligned to the Ensemble genome references Coturnix_japonica_2.0 (GCA_001577835.1) or GRCg6a (GCA_000002315.5) for quail or chicken libraries, respectively. Alignment was performed using STAR version 2.5.0 with the following options: –outFilterType BySJout –alignSJoverhangMin 8 –alignSJDBoverhangMin 5 –alignIntronMax 100000 –outSAMtype BAM SortedByCoordinate –twopassMode Basic –outFilterScoreMinOverLread 0 –outFilterMatchNminOverLread 0 –outFilterMatchNmin 0 –outFilterMultimapNmax 1 –limitBAMsortRAM 10000000000 –quantMode GeneCounts (Dobin et al., 2013). Gene counts were determined using the htseq-count function from HTseq (version 0.9.1) (Anders et al., 2015) in union mode and discarding low quality score alignments (–a 10), using the Ensembl Coturnix_japonica_2.0 or GRCg6a genome annotations. On average, 67% and 77% of the filtered reads from quail and chicken samples mapped to a single genomic location, corresponding to ~14 500 and ~15 400 detected genes, respectively. *Dataset 1* presents the summary information of the RNA-seq datasets.

Clustering of normalized gene counts and Principal Component Analysis (PCA) for exploratory data analysis were performed with the pheatmap R package using the euclidean distance matrix computation of the dist function, and the ggfortify:plotPCA function, respectively.

Differential Expression Analysis (DEA) for RNA-Seq gene counts was performed with the limma Bioconductor package using the voom method to convert the read-counts to log2-cpm, with associated weights, for linear modeling (Law et al., 2014; Ritchie et al., 2015). Differential gene expression analysis was performed by making all possible comparisons between the three *C. japonica* experimental conditions or by comparing the two *G. gallus* experimental conditions, using all available replicate data. Genes showing up or down-regulation with an adjusted *p value* <0.01 and a log2 fold change (log2FC) of |log2FC|>0.6 were considered differentially expressed.

GO analysis to elucidate potential biological processes associated to up-regulated genes was performed using inBio Discover (T. Li et al., 2017) and g:Profiler (Reimand et al., 2007).

Heatmaps for differentially expressed genes were generated using the pheatmap function from the R pheatmap package with the ward.D or complete clustering method, for all genes or only transcription factors, respectively.

Functional Enrichment Analysis

Functional annotations were downloaded from Ensembl Genes 105 for the quail (Coturnix_japonica_2.0) and chicken (GRCg6a) genes using the integrated Biomart interface. Functional enrichment of differentially expressed genes was performed with the GOfuncR package version 1.14.0 using all the detected genes in our dataset as background and the core function goenrich with default parameters (hypergeometric test, 1000 randomizations), considering as significant as FDR < 0.01.

Identification and Classification of the Differentially Expressed Genes

For the identification of the differentially expressed genes, for which the Ensembl genome annotation did not provide a Gene Symbol alias (422 genes), the correspondent ENSEMBL gene ID was manually searched in Ensembl and NCBI Gene resources. When this approach did not identify a match, the Ensembl Database was searched for highly similar sequences using BLAST alignment and the gene symbol for the top scoring gene alignment was used as alias. Genes functions were further studied using the respective bioinformatic platforms: Ensembl (Kuleshov et al., 2016), GEISHA (Gallus Expression In Situ Hybridization Analysis, Darnell et al., 2007), MGI (Mouse Genome Informatics, Bult et al., 2019), UniProtKB , g:Profiler (Reimand et al., 2007) and Enrichr (Kuleshov et al., 2016).

4
RESULTS AND DISCUSSION

This section is a modified version of the correspondent one found in:
Isabel Alcobia, Margarida Gama-Carvalho, Leonor Magalhães, Vitor Proa, Domingos Henrique, Hélia Neves (2022). *Thymus formation in uncharted embryonic territories.* Available in BioRxiv doi:10.1101/2022.03.09.483697 https://biorxiv.org/cgi/content/short/2022.03.09.483697v1

GENERAL FUNCTIONAL ASSAYS RESULTS – ENDODERM AND MESENCHYME DERIVATIVES

The first results of this study were obtained after extensive histological analysis of explants derived from associations of PP endoderm and mesenchyme. For this process, I've learned to identify and characterize all embryonic tissues grown in the explants. Besides the major focus on thymus and PT glands formation, and as expected, associations derived explants originated several other embryonic tissues/organs (Figure 8). Namely, all the associations of endoderm from different PP (1PP, 2PP, 3/4PP) presented the thyroid gland (Figure 8a). During the isolation procedure, thyroid rudiment was intentionally kept in the dissected endoderm, to be used as a quality control for endoderm development *in vitro* and *in ovo*. Additionally, simple columnar to simple cuboidal epithelium were found in the samples, revealing the initial developmental stages of the future digestive and respiratory tract epithelium, respectively. Caliciform cells were also identified in these epithelia. All epithelial cells (except for vessels) derived from quail endoderm ($QCPN^+$ cells). Most of the samples displayed eosinophilic infiltrate (Figure 8b), as well as cartilage (Figure 8d). Other recurrently recognized tissues were bone (Figure 8c), smooth muscle (Figure 8e), skeletal muscle, and specialized conjunctive tissue derived from chicken tissues ($QCPN^-$ cells). These results showed the capacity of associated tissues (endoderm and mesenchyme) to differentiate *in vitro* and *in ovo*. Occasionally, feathers ($QCPN^+$ cells) were also identified revealing some ectoderm contamination during endoderm isolation procedure (Figure 8f).

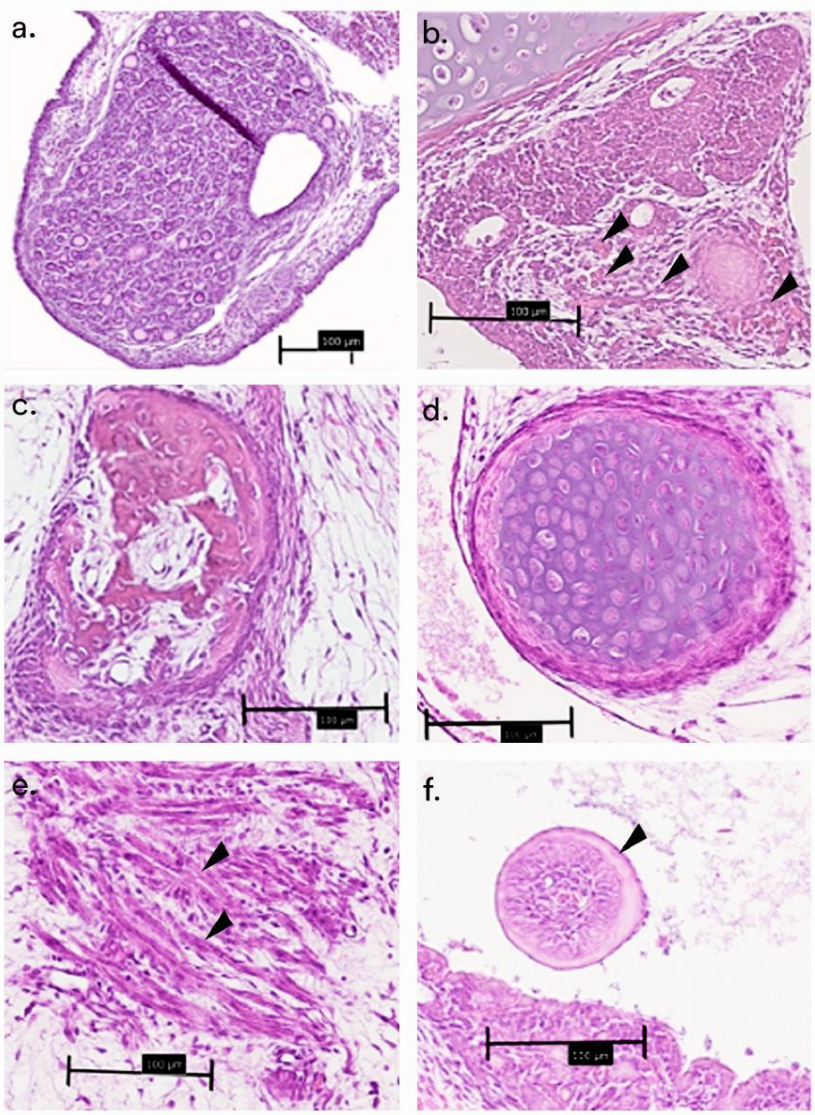

Figure 8. Sections of embryonic tissues and organs found in heterospecific associations explants (H&E stain). Heterospecific associations supported the development of several embryonic tissues/organ, such as thyroid gland (a); eosinophil cells (b, arrowheads); bones (c); cartilage (d); smooth muscle (e, arrowheads) and feathers (f, arrowhead). Scale bars, 100µm.

ENDODERM FROM DIFFERENT PHARYNGEAL POUCHES CONSERVES THYMIC POTENTIAL

The 2PP endoderm has similar thymic potential to the 3/4PP endoderm

During chicken embryonic development, TE derives from the 3/4PP endoderm (canonical pouch). To evaluate the capacity of non-canonical pouches to form a thymus, we started by removing them from their natural environment and associate with a permissive mesenchyme, the somatopleura mesoderm (SM) (in Materials and Methods, Figure 7). The SM capacity to support thymus development at ectopic locations in the embryo was previously demonstrated when grafting 3/4PP endoderm into the body wall of a chicken embryo (Le Lièvre & Le Douarin, 1975; Neves, Dupin, Parreira, & Le Douarin, 2012).

Using a modified chick-quail chimera system, 2PP endoderm was isolated from quail (q) embryos at E3 and *in vitro* associated with chicken (c) E2,5 SM, for 48h (Figueiredo & Neves, 2019; Neves, Dupin, Parreira, & Le Douarin, 2012). To evaluate the capacity of this heterospecific association to form a thymus, the 48h-cultured tissues were then grafted into the chorioallantoic membrane (CAM) of a chicken embryo (E8) and allowed to develop *in ovo* for further 10 days (Figueiredo et al., 2016; Figueiredo & Neves, 2018; Figure 7). The CAM behaves as a vascular supplier of nutrients and allows gas exchanges to grafted tissues, enabling their development *in ovo* for longer periods of time. In parallel, associations of 3/4PP endoderm (qE3) with SM (cE2,5) were used as positive control.

Morphological analysis of tissues formed in CAM-explants was performed by conventional histology and immunohistochemistry, as previously described (Figueiredo et al., 2016; Figueiredo & Neves, 2018). Endoderm-derived cells were identified by immunohistochemistry using quail-specific antibody, mAb Quail PeriNuclear (QCPN).

Similar to control associations of 3/4PP endoderm, the 2PP endoderm-derived CAM-explants contained fully formed chimeric thymus with cortical and medullary compartments (Figure 9a and Figure 9d). Quail-derived thymic epithelium displayed a reticular architecture (QCPN+, Figure 9b and Figure 9e) and it was colonized by lymphoid progenitor cells of donor origin (chicken) (Figure 9c and Figure 9f). The presence of CD3+ T-lymphocytes was also confirmed in these ectopic thymic structures. Considering pairwise developmental stage (qE12 and cE15), one in four lymphoid cells of chimeric

thymus should express the CD3 marker (data not shown, results from Carlota Lucena Master thesis; Ainsworth et al., 2010). Similar CD3+ cell numbers were observed in chimeric thymus from 2PP or 3/4PP endoderm-derived CAM-explants (Figure 9c and Figure 9f).

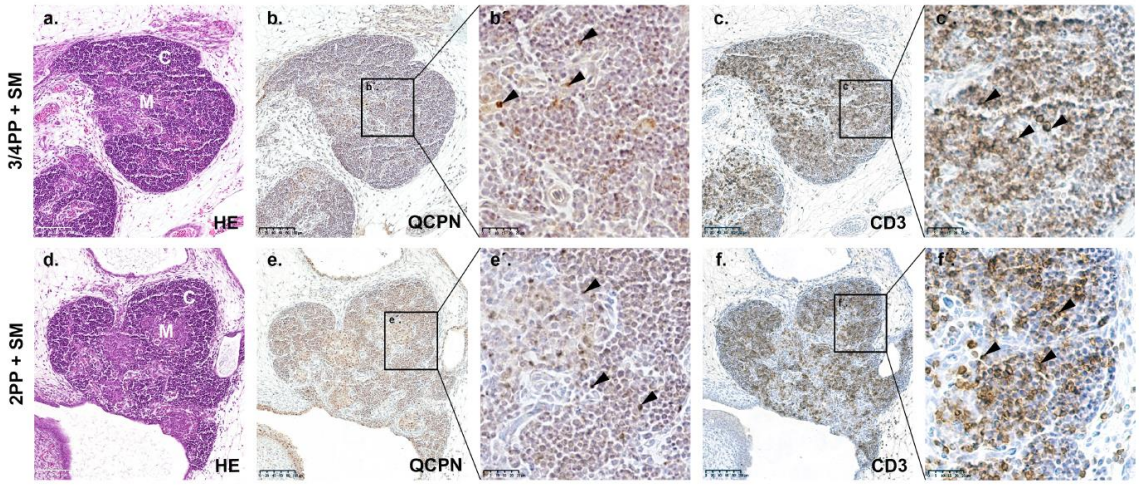

Figure 9. Thymus formation in CAM-derived explants of PP endoderm and somatopleura mesoderm associations. Serial sections of thymi stained with H&E (a and d), and immunodetected with QCPN (quail cells) (b and e) and CD3 (T-cells) (c and f) antibodies. *Top panel (a-c)* - Thymus derived from associations of quail 3PP endoderm with chicken SM. *Bottom panel (d-e)* - Thymus derived from associations of quail 2PP endoderm with chicken SM. Arrowheads point immunostaining positive cells for QCPN (quail thymic epithelium) and for CD3 (chicken T-cells differentiated in the thymus). CAM, Chorioallantoic Membrane; PP, Pharyngeal Pouch; SM, Somatopleura Mesoderm. Scale bars, 100µm.

The 2PP endoderm-derived CAM-explants with a fully formed thymus (n=6/6) were identical to those obtained when canonical 3/4PP was tested under the same conditions (n=5/5) (Table 1).

Heterospecific association of tissues	2PP endoderm	3/4PP endoderm
Somatopleura mesoderm	6/6	5/5
3/4 PA mesenchyme	3/3	3/3
2 PA mesenchyme	ND	2/3
2 PA mesenchyme - Ventral territory	ND	3/3
2 PA mesenchyme - Dorsal territory	ND	1/5

Table 1. Chimeric thymus in CAM-explants. Number of samples with thymus per total number of samples. ND, Not Done; PP, Pharyngeal Pouch; PA, Pharyngeal Arch

As demonstrated, the 2PP endoderm is capable of forming a fully arranged and functional chimeric thymus in similar way as 3/4PP endoderm, when exposed to same permissive mesenchymes. These results point to the existence of a conserved program to form a thymus embodied in the endoderm of different PPs, independently of their specific anatomical location.

Remarkably, the 2PP endoderm-derived explants also gave rise to parathyroid glands (n=4/6; Table 2), suggesting an extended conservation mechanism in the formation of both organs, within distinct pouches.

Heterospecific association of tissues	2PP endoderm	3/4PP endoderm
Somatopleura mesoderm	3/6	2/5
3/4 PA mesenchyme	0/2	3/3
2 PA mesenchyme	ND	2/2
2 PA mesenchyme - Ventral territory	ND	2/3
2 PA mesenchyme - Dorsal territory	ND	5/5

Table 2. Chimeric parathyroids in CAM-explants. Number of samples with parathyroids per total number of samples. ND, Not Done; PP, Pharyngeal Pouch; PA, Pharyngeal Arch

Still, no thymus was formed when 1PP endoderm was associated with SM. Only small epithelial clusters were observed (n=5/6), with scarce CD3+ cells, suggesting a residual potential of this pouch endoderm to develop a thymic-like epithelium (Figure 10).

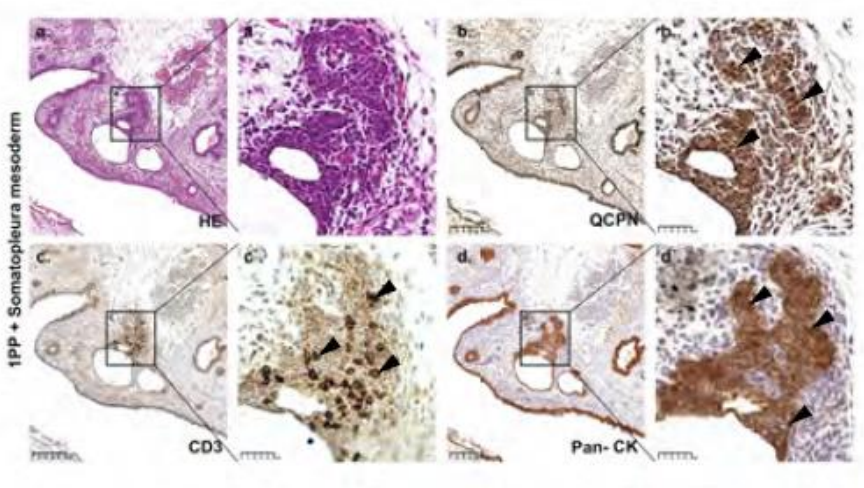

Figure 10. Lymphoid clusters in CAM-derived explants of 1PP endoderm and Somatopleura mesoderm associations. Serial sections of thymi stained with H&E (a), and immunodetected with QCPN (quail cells) (b), CD3 (T-cells) (c) and anti-pan cytokeratin (CK) antibody (epithelial cell marker) (d) antibodies. Lymphoid clusters derived from associations of quail 1PP endoderm with

chicken SM. Arrowheads point immunostaining positive cells for QCPN (quail thymic epithelium) and for CD3 (chicken T-cells differentiated in the thymus). CAM, Chorioallantoic Membrane; PP, Pharyngeal Pouch; SM, Somatopleura Mesoderm. Scale bars, 100µm.

The 2PP and 3PP endoderm share a conserved genetic program

Considering the capacity of 2PP endoderm to give rise to thymus epithelium, we then asked if this endoderm tissue could share a common genetic program with the 3/4PP endoderm.

To evaluate this, the anterior endoderm region at qE3 was isolated (Figueiredo & Neves, 2019; Neves, Dupin, Parreira, & Le Douarin, 2012) and separated in three regions (Figure 11a): 2PP, 3/4PP and the central territory of anterior endoderm (pharynx), the latter as a negative control to thymic potential. Total RNA was isolated from three biological replicate samples of each region and used to generate libraries for Illumina paired-end mRNA-seq. High quality sequencing datasets were obtained for all samples, with an average 7 million reads mapping uniquely to the quail genome, corresponding to the detection of ~14 500 genes (*Dataset 1*).

Analysis of this dataset identified the differentially expressed (DE) genes between the three tissues (Figure 11b). In general evaluation and as expected, a greater similarity of transcription profiles is displayed between the 3/4PP and 2PP, when compared with the central portion of the pharynx endoderm (Figure 11b).

In particular, comparing the pouches' endoderm to pharynx, 492 and 555 up-regulated transcripts (log2FC >0.6, adj pval <0.01) were detected in 3/4PP and 2PP endoderm, respectively (Figure 11c and Figure 11d; the complete list of DE genes can be found in *Dataset 2*). Each group of the above upregulated transcripts, 41 (of 492 genes in 3/4PP endoderm) and 56 (of 555 genes in 2PP endoderm) did not display Gene Symbol, which was then manually search (see Material and Methods).

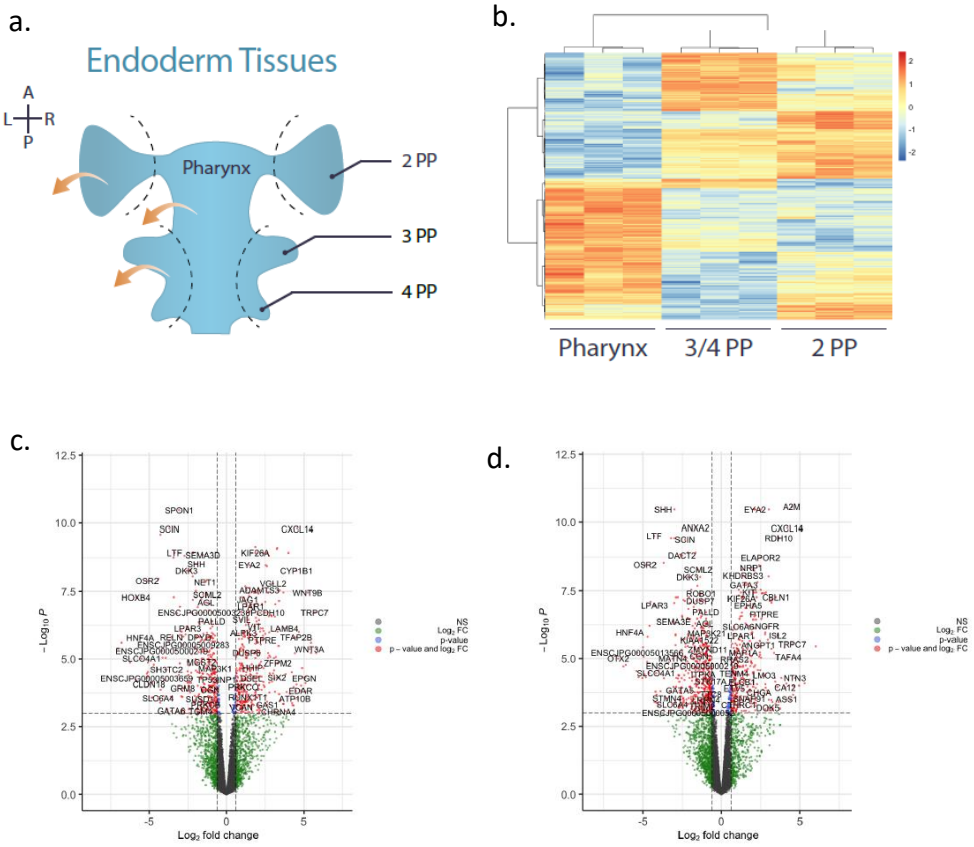

Figure 11. Transcriptional profiles of isolated pharyngeal endoderm tissues. a) Schematic representation of distinct endoderm tissues isolated from the embryonic pharyngeal region at qE3. b) Heatmap showing differentially expressed genes in the pharynx, 3/4PP and 2PP endoderm (Log2 Fold Change (FC) >0.6 and <−0.6, and P-value <0.01). c) and d) Volcano plots depict differentially expressed transcripts of 3/4PP and 2PP, respectively, comparing with the pharynx. Red dots highlight transcripts passing the log2FC and adj pvalue cut-offs and blue dots highlights transcripts with adj pval <0.01. A, Anterior; L, Left; P, Posterior; PP, Pharyngeal Pouch; R, Right.

Of these, 262 transcripts were commonly up-regulated in both 2PP and 3/4 PP pouches, with 31 of these genes annotated as encoding Transcription Factors and Regulators (TF&R) (Figure 11c-d and Figure 12).

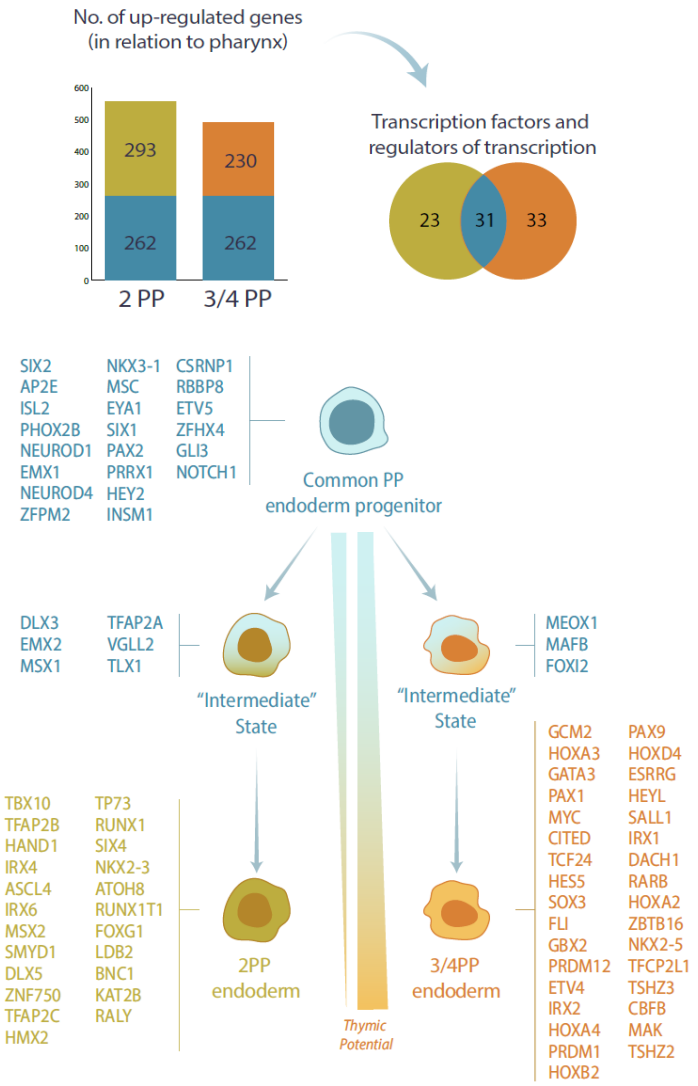

Figure 12. Schematic representation of the genetic profile of distinct PP progenitors. The enrichment of up-regulated transcription factors and regulators when comparing PPs with the pharynx. Schematic view of a cascade of transcription profiles as the common PP endoderm progenitor increases in thymic potential. PP, Pharyngeal Pouch

A closer examination uncovered 31 up-regulated transcripts encoding Transcription Factors and Regulators (TF&R) common to PP endoderm (Figure 12). Considering the ability shown by the 2PP endoderm to mimic 3/4PP endoderm developmental potential, the set of commonly enriched transcripts should reflect a shared genetic program regulating the establishment of a *general PP endoderm progenitor population* (Figure 12). One may wonder if a conserved thymic potential is embodied within this genetic

program. In effect, various of these up-regulated transcripts encodes TF&Rs that have been shown to play crucial roles in early stages of T/PT organogenesis in mouse, chicken and human, namely EYA1/SIX1 (X. Li et al., 2003); and Figure 6) and NOTCH1/GLI3 (Figueiredo et al., 2016; and Figure 6). Figueiredo *et al* demonstrated that Notch signalling operates in a Hh-dependent manner during early development of T/PT common primordium. The most evident expression of GLI3 (Hedgehog target gene), *in situ*, was found in dorsal tip of the 3PP endoderm, at E3-E4 (Figueiredo et al., 2016). NEUROD1, another up-regulated transcription factor that was recently found to be expressed in later stages of thymic development, by neuroendocrine cells, a subset of mTEC (Bautista et al., 2021; Park et al., 2020).

In addition, we found 3 transcripts encoding other TF&Rs, MEOX1, MAFB and FOXI2, which, despite being common to both PP, show higher expression in 3/4PP endoderm when compared to 2PP endoderm. This suggests the existence of an *"intermediate" stage of commitment* into 3/4PP endoderm, starting from the common progenitor (Figure 12). MABF and MEOX1 were mainly identified in parathyroid development. MABF has been described to regulate later steps on parathyroid development, mainly in PT separation and migration from the thymus. MAFB is also involved in PTH secretion, acting synergically with Gcm2, by binding to PTH promoter (Kamitani-Kawamoto et al., 2011; Magaletta et al., 2022). MEOX1 is classically known to be required for somitogenesis, especially sclerotome formation, and for vascular cell proliferation regulation (Nguyen et al., 2014; Reijntjes et al., 2007). FOXI2 was shown to be expressed in PA mesenchyme of chicken embryos (Khatri & Groves, 2013).

Conversely, we found 6 transcripts encoding TF&Rs with higher expression in 2PP endoderm (DLX3, EMX2, MSX1, TFAP2A, VGLL and TLX1), which might pinpoint to a similar *"intermediate" stage of commitment* into 2PP endoderm (Figure 12). Interestingly, TFAP2A acts up-stream of MSX1 and MAFB in neural crest progenitors (Enkhmandakh & Bayarsaihan, 2015), and mutations in this gene cause branchio-oculo-facial syndrome.

Lastly, our data also revealed the existence of a set of 23 transcripts encoding TF&Rs up-regulated in 2PP versus 3/4PP endoderm, and 33 TF&Rs upregulated in 3/4PP versus

2PP (Figure 12 and Figure 13). These two gene-sets may represent a further step into the gene cascade that regulates the acquisition of 2PP and 3/4PP identities.

Several up-regulated transcripts in 3/4PP endoderm encode TF&Rs like GCM2, HOXA3, GATA3, PAX1 and PAX9, which are known to be crucial in 3/4PP patterning and T/PT common primordium specification in various animal models (reviewed by Figueiredo et al., 2020; and Figure 6). Other transcripts, encoding TF&Rs HOXA2, NKX2-**5**, MYC, GBX2, SALL1 and PRDM1, were recently detected in immature pharyngeal cells and thymic epithelium progenitors (Magaletta et al., 2022). In particular, NKX2-5 acts as a Foxn1-independent early marker of thymus fated cells, having its expression restricted to the endoderm of the presumptive thymic domain, at mE10.5 (Wei & Condie, 2011). GBX2 is required for normal arch artery development (specially 4PA artery), as null GBX2 mutant displays similar cardiovascular defects to DiGeorge Syndrome - TBX1 mutation phenotype (Calmont et al., 2009; Ivins et al., 2005). GBX2 was recently described to be a downstream of TBX1 and PAX9. The three genes are expressed in the pharyngeal endoderm at E9.5 and E10.5, in mice (Stothard et al., 2020).

We note a strong enrichment of transcripts encoding Hox genes in the 3/4PP endoderm, when compared to 2PP endoderm (Figure 13). Hox (Homeobox) genes are a cluster of transcription factors responsible for positional identity along the Anterior-Posterior axis of the embryo. Specific combinations of Hox-genes code define the distinct regions on AP-axis (Gordon, 2018). Besides the well described HOXA3 (reviewed by Figueiredo et al., 2020), the enrichment in Hox genes (HOXA2, HOXA4, HOXB2, HOXD4) suggests the existence of a specific Hox boundary at the interface between the second and third/fourth pharyngeal arches, likely important to define the identity of each pouch.

Finally, we detected up-regulation of three Notch-targets transcripts in 3/4PP endoderm, HEYL, HES5, and the already mentioned GATA3, pointing to an overlooked involvement of Notch activity in these early stages of thymus organogenesis (Figueiredo et al., 2016; Figure 12 and Figure 13).

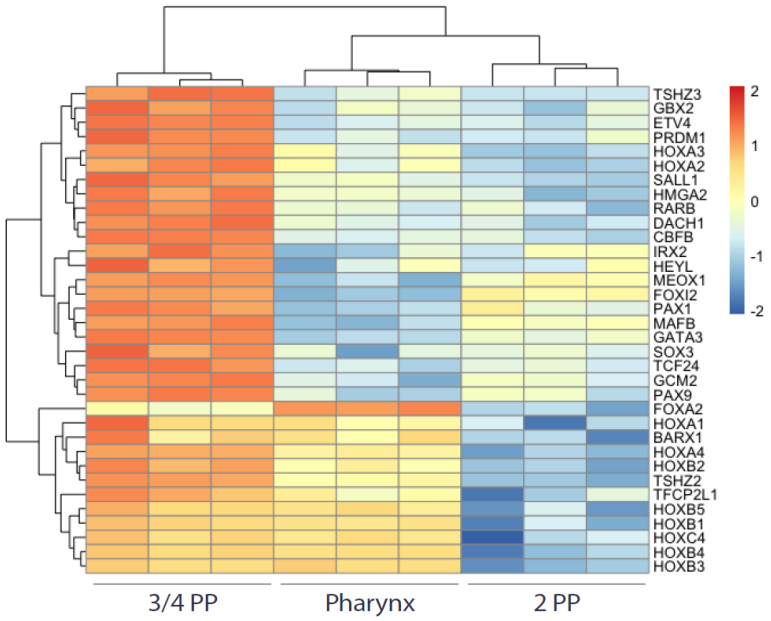

Figure 13. Heatmap of Transcription Factors and Regulators Differentially Expressed in the pharyngeal endodermal tissues. Depicts the most up-regulated transcripts in 3/4PP (Log2FC >0.6 and <−0.6, and P-value <0.01, and P-value <0.01). PP, Pharyngeal Pouch.

The genetic signature of prospective thymic rudiment in 3/4PP endoderm.

While the previous analysis focused on examining gene expression changes that might underlie the initial acquisition of a thymic potential in the PP endoderm, understanding how thymus development is restricted to the 3/4PP endoderm might be better approached by directly comparing the transcriptomes of the 2PP and 3/4PP endoderm.

This analysis revealed that 165 transcripts are upregulated in 3/4PP endoderm when comparing with 2PP endoderm, whereas 353 transcripts are downregulated (Figure 14a-b, and *Dataset 2*). From the total 518 transcripts, only 31 were manually searched for Gene Symbol (see Material and Methods).

inBio Discover analysis of these differentially expressed genes revealed GO-term enrichment mainly in morphogenesis and vascular development (Figure 14c). This analysis also revealed an association of 2PP endoderm up-regulated genes with GO-terms of negative regulation of developmental processes (Figure 14c).

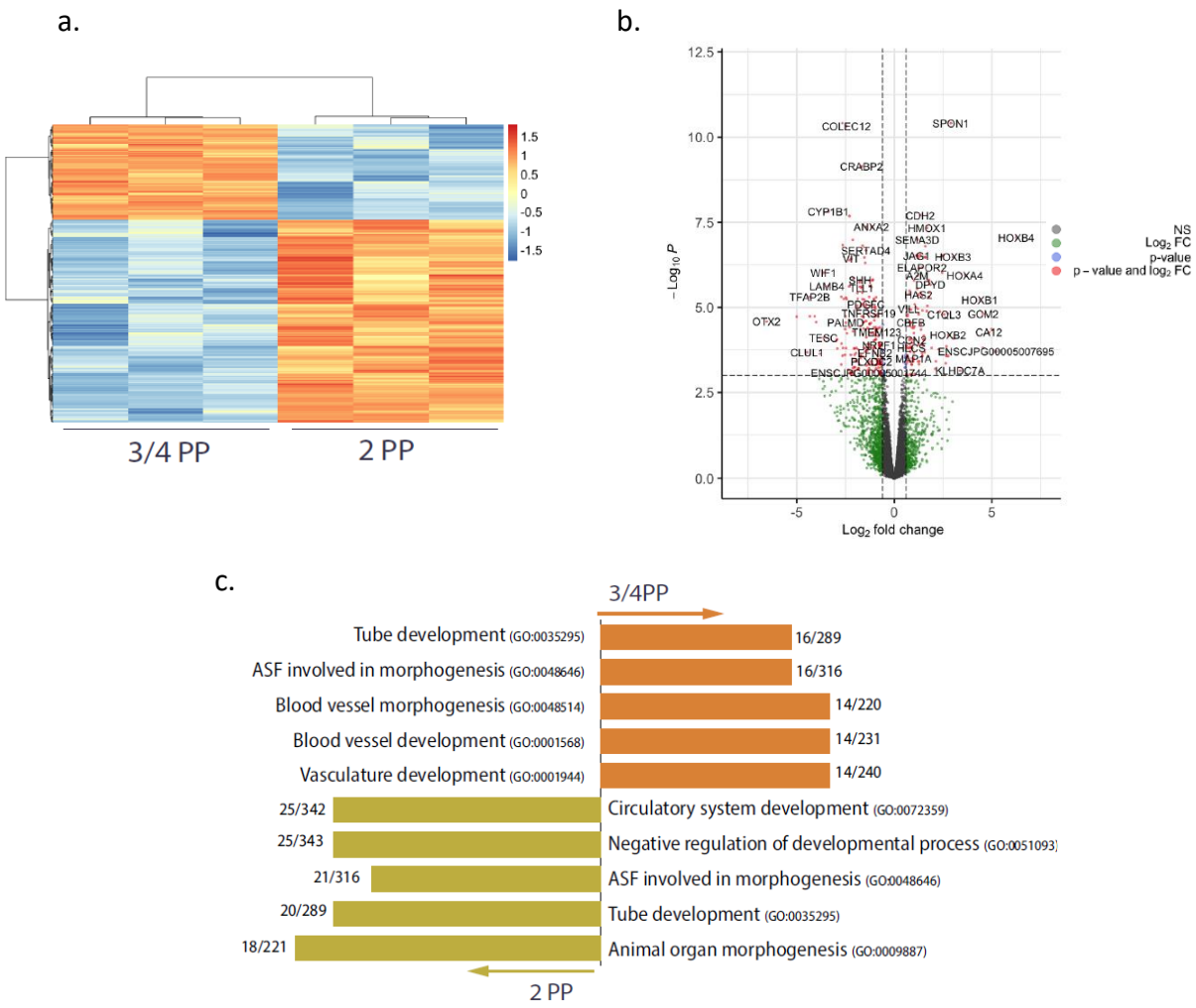

Figure 14. Differential gene expression analyses reveal discrete transcriptomic signature of 2PP and 3/4PP endoderm. a) Heatmap showing differentially expressed genes in 3/4PP and 2PP endoderm (Log2FC >0.6 and <−0.6, and P-value <0.01). b) Volcano plot depicts differentially expressed transcripts of 3/4PP endoderm comparing with the 2PP endoderm. Red dots highlight transcripts passing the log2FC and adj pvalue cut-offs and blue dots highlights transcripts with adj pval <0.01. c) Bar plot depicting inBio Discover analysis of Top 5 Gene ontology (GO) – Bio.Process for 518 genes differentially expressed in 3/4PP and 2PP endoderm. ASF, Anatomical structure formation; PP, Pharyngeal Pouch.

Functional gene annotation identified 34 transcripts encoding TF&Rs specifically up-regulated in 3/4PP endoderm. 10 of these encode HOX TFs (Figure 14b and Figure 15), and this strong enrichment in Hox gene expression in 3/4PP endoderm reinforces the hypothesis that there is a clear identity boundary between 2PP and 3/4PP, probably critical for correct thymus specification. Indeed, HOXA2 and HOXA3 have been associated to T/PT formation, and HOXB1, HOXB2, HOXB4 and HOXB5 were recently associated to ultimobranchial body formation in mouse 4PP endoderm (Magaletta et al.,

2022). Of the remaining 24 up-regulated TF&Rs in 3/4PP endoderm, SOX3 was shown to be required for PP formation and consequently to craniofacial morphogenesis (Rizzoti & Lovell-Badge, 2007).

The analysis of TF&R genes in 2PP endoderm revealed a set of 40 up-regulated transcripts (Figure 14b and Figure 15). Of these, GRHL3, TP63, TFAP2A, MSX1, MSX2, TBX10, DLX5 and SOX9 are known to be involved in orofacial cleft disease (Reynolds et al., 2019, 2020). Namely, GRHL3 was found to be a putative new transcriptional regulator of the medullary thymic epithelial sub-lineage (Park et al., 2020; Magaletta ME et al., 2022).

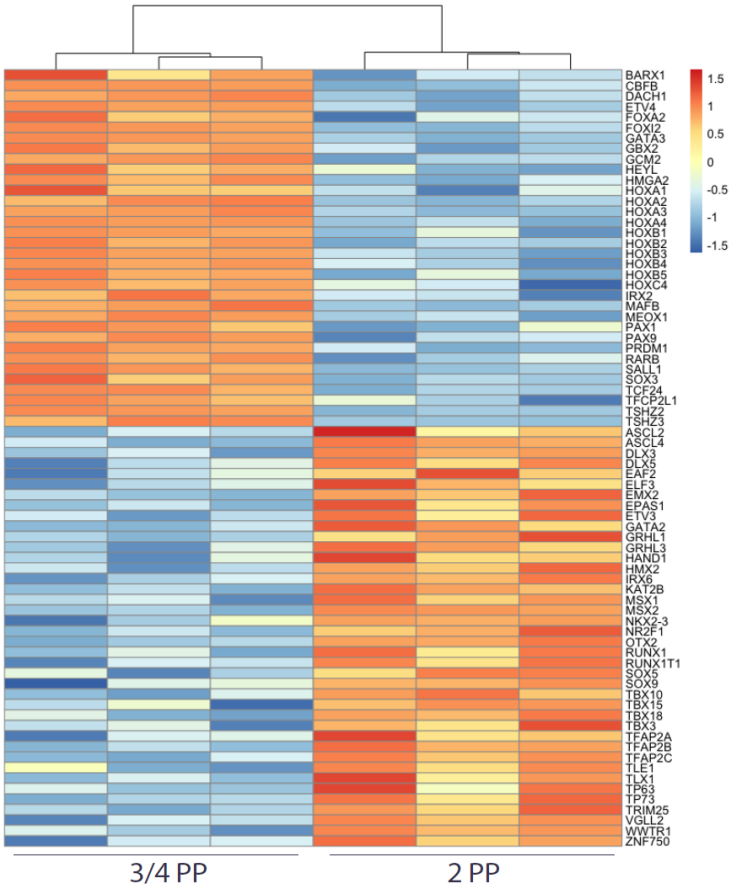

Figure 15. Transcriptomic Signature of 3/4PP and 2PP endoderm. a) Heatmap showing the selected transcription factors and regulators differentially expressed in 3/4PP and 2PP endoderm (log2FC >0.6 and <−0.6, and P-value <0.01). PP, Pharyngeal Pouch.

MESENCHYME FROM PHARYNGEAL ARCHES REGULATES THYMIC FORMATION

The mesenchyme of the PA modulates thymic potential of PP endoderm.

The capacity of 2PP endoderm to form a thymus when associated with ectopic mesenchyme reveals not only the thymic potential in this region but also that signals from adjacent PA mesenchyme are important to regulate such potential in PP endoderm. The fact that 2PP does not normally give rise to thymus might indicate that the underlying 2PA mesenchyme is unable to promote thymus development, or that it can even provide a local repressive environment for thymus formation. Conversely, the mesenchyme of 3/4 PA is expected to produce signals that promote thymus formation in the overlying endoderm.

To test these hypotheses, 2PP endoderm was isolated from chicken embryos and associated *in vitro* with 3/4 PA mesenchyme, followed by growth *in ovo*, as described above. As expected, thymus was formed in 2PP endoderm-derived CAM-explants (n=3/3; Table 1) with the typical thymic characteristics (Figures 16a-c). Similarly, thymus was formed in 3/4 PP and 3/4PA associations (n=3/3, Figures 16d-f, Table 1). These results confirm the capacity of 3/4PA mesenchyme to promote thymus development.

To test for the presence of thymus-repressive signals in 2PA mesenchyme, this was associated with 3/4PP endoderm. Surprisingly, normal thymus was formed in CAM-explants derived from these associations (n=3/3, Figures 16g-l, Table 1). Considering that thymic rudiments in chicken embryos emerge at the dorsal domain of 3/4PP, we asked whether the mesenchyme of the arches could have regionalized properties along the dorso-ventral axis. The 2PA mesenchyme was isolated and further sectioned into dorsal (2PAd) and ventral (2PAv) regions, by microsurgical procedures (Figueiredo & Neves, 2019). These sub-regions were then associated with 2PP or 3/4PP endoderm. CAM-explants derived from 3/4PP endoderm and 2PAv mesenchyme associations displayed normal thymus formation (n=3/3, Figures 16j-l, Table 1). Conversely, only one in six CAM-explants presented thymus when 3/4PP endoderm was associated with 2PAd mesenchyme, revealing its inhibitory properties for thymus formation. This property seems restricted to thymus potential, as parathyroid glands develop in the presence of 2PAd mesenchyme (n=5/5, Table 2). Of notice, the 1PA mesenchyme also showed

permissive properties to thymus formation. Tissue associations of 3/4PP endoderm with 1PA mesenchyme were able to form a thymus (n=5/6).

Together, these results show that the local mesenchyme of the pharyngeal arches regulates the potential thymic outcome in distinct pouches.

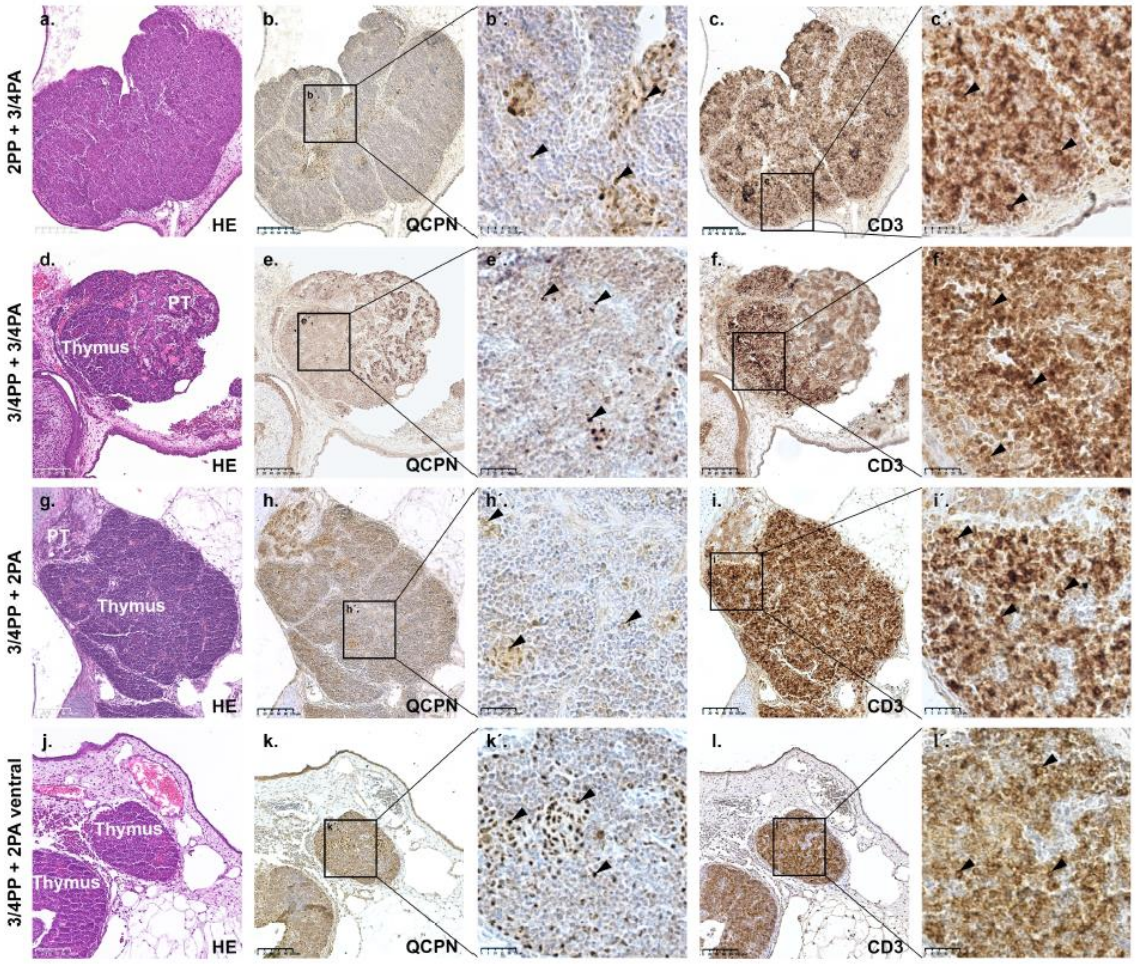

Figure 16. Thymus formation in CAM-derived explants of PP endoderm and mesenchyme associations. Serial sections of thymi stained with H&E (a, d, g and j), and immunodetected with QCPN (quail cells) (b, e, h and k) and CD3 (T-cells) (c, f, i and l) antibodies. *First panel (a-c)* - thymus derived from associations of quail 2PP endoderm with chicken 3/4PA mesenchyme. *Second panel (d-f)* - thymus derived from associations of quail 3/4PP endoderm with chicken 3/4PA mesenchyme. *Third panel (g-i)* - thymus derived from associations of quail 3/4PP endoderm with chicken 2PA mesenchyme. *Fourth panel (j-l)* - thymus derived from associations of quail 3/4PP endoderm with chicken ventral territory of 2PA mesenchyme. Arrowheads point immunostaining positive cells for QCPN (quail thymic epithelium) and for CD3 (chicken T-cells differentiated in the thymus). CAM, Chorioallantoic Membrane; E, Embryonic day; PA, Pharyngeal Arch; PP, Pharyngeal Pouch; PT, Parathyroid gland. Scale bars, 100µm.

PA mesenchymal signals that regulate PP thymic potential.

To unravel the mesenchyme-derived signals that modulate thymus formation, we performed an unbiased, in-depth transcriptome analysis of isolated mesenchymal tissues from distinct PAs at cE2.5: 3/4PA, corresponding to a microenvironment favouring thymus formation; and the dorsal region of 2PA (2Pad), which we demonstrated as having inhibitory properties to thymus development (Figure 17a). Total RNA was isolated from three biological replicate samples from the two regions and mRNA libraries were generated for paired-end illumina sequencing. High quality RNA-seq datasets were recovered for all samples, with an average of 7.7 million reads mapping uniquely to the *Gallus gallus* genome, corresponding to an average detection of ~15 400 genes (*Dataset 1*).

Of these, 532 transcripts were found to be differentially expressed between 3/4PA and 2PAd with a log2FC >0.6 (adj pval <0.01) (Figures 17b-c, a complete list of genes in *Dataset 2*). From these 532 transcripts, 294 transcripts needed the Gene Symbol to be searched (see Material and Methods).

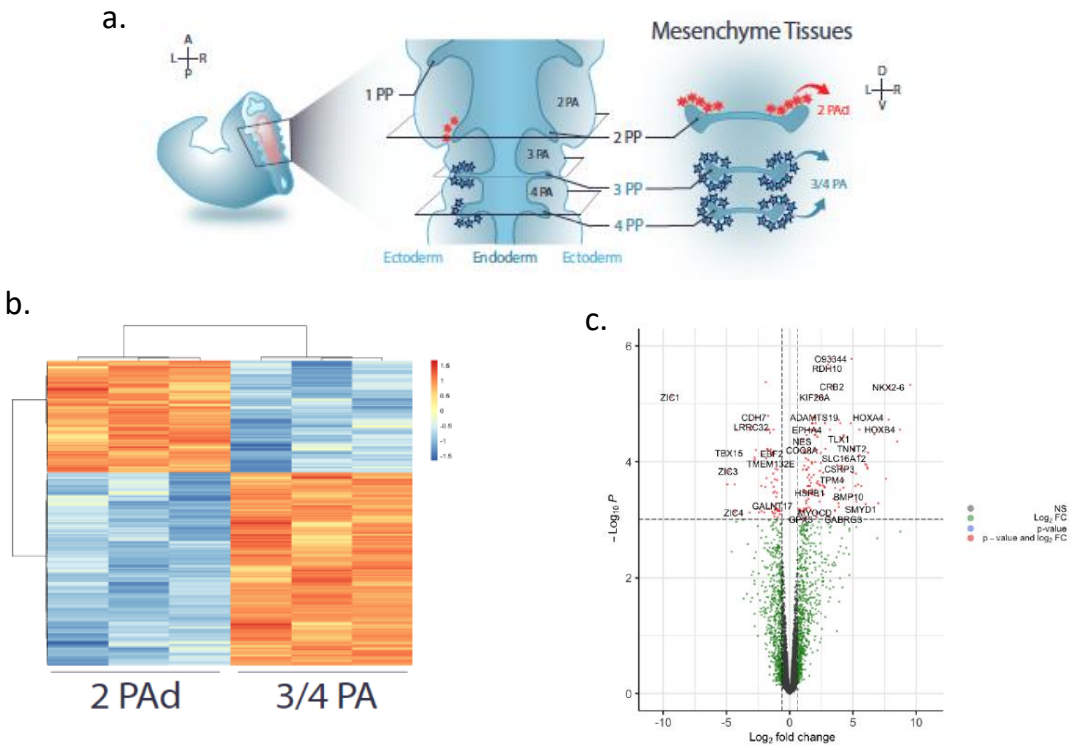

Figure 17. Transcriptional profiles of pharyngeal mesenchyme tissues. a) Schematic representation of distinct mesenchyme tissues isolated from the embryonic pharyngeal region at qE3. b) Heatmap showing differentially expressed genes in the 2PAd and 3/4PA (fold change >0.6 and <−0.6, and P-value <0.01). c) Volcano plot depicts differentially expressed transcripts

of 3/4PA comparing with 2PAd. Red dots highlight transcripts passing the log2FC and adj pvalue cut-offs and blue dots highlights transcripts with adj pval <0.01. A, Anterior; D, Dorsal; L, Left; P, Posterior; PA, Pharyngeal Arch; PAd, Pharyngeal Arch - dorsal territory; PP, Pharyngeal Pouch; R, Right; V, Ventral.

The inBio Discover analysis of Top 5 Gene ontology (GO) – Bio.Process of the 317 upregulated genes in 3/4PA mesenchyme, revealed an enrichment in GO-terms related to vascular development processes (Figure 18). Similar results were obtained for the 176 upregulated genes in 2PAd mesenchyme. Still, an enrichment in GO-terms related to epithelial to mesenchymal transition (EMT) processes was also identified for these transcripts (Figure 18).

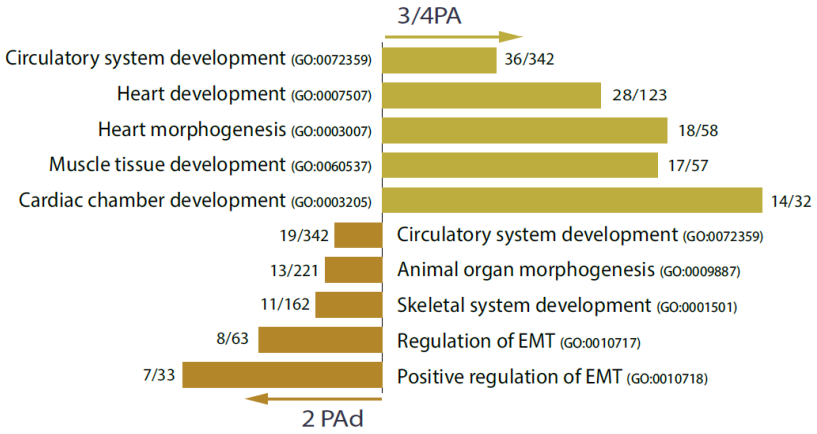

Figure 18. Bar plot depicting inBio Discover analysis of Top 5 Gene ontology (GO). Bio.Process for 317 genes differentially expressed in 3/4PA mesenchyme versus 2PAd mesenchyme. EMT, Epithelial to Mesenchymal Transition; PA, Pharyngeal Arch; PAd, Pharyngeal Arch - dorsal territory.

A detailed inspection of major signalling pathways (VEGF, Retinoid Acid, BMP, Wnt, Notch, EPH-Ephrin, FGF and Hedgehog) was also performed (Figure 19a and Table 3). We found a clear difference in gene enrichment for distinct signalling pathways when the two tissues were compared. All the major signalling pathways, with exception for Wnt, were enriched in the 3/4PA when compared to 2PAd (Table 3).

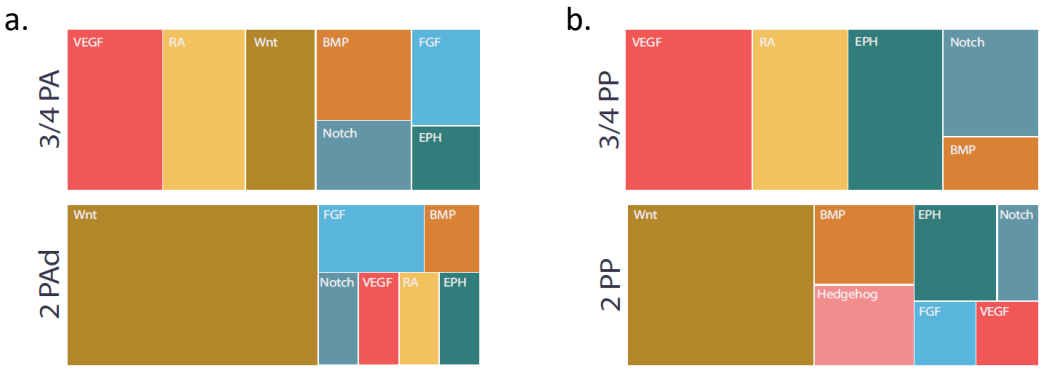

Figure 19. Treemaps depict up-regulated transcripts of major signalling pathways. VEGF, Retinoid Acid, BMP, Wnt, Notch, EPH-Ephrin, FGF and Hedgehog expression in 3/4PA vs 2Pad (a) and 3/4PP vs 2PP (b). PA, Pharyngeal Arch; PP, Pharyngeal Pouch; RA, Retinoic Acid.

As expected, several transcripts for BMP ligands were up-regulated in the 3/4PA mesenchyme (Bleul & Boehm, 2005; Gordon et al., 2010; Jerome-majewska et al., 2002; Neves, Dupin, Parreira, & Le Douarin, 2012; Patel et al., 2006), when compared to 2PAd mesenchyme. Namely, one of BMP ligands detected was BMP4. In avian model, BMP4 expression by mesenchymal cells adjacent to 3/4PP is necessary for early development of thymic and PT rudiments from these PP. This mesenchymal expression is limited in time and maintained until the endoderm of these PP starts expressing BMP4. This is a good example of one of many epithelial-mesenchyme interactions occurring in thymus development (Neves, Dupin, Parreira, & Le Douarin, 2012). Interestingly, the only transcript from the BMP pathway found upregulated in 2PAd was CHRDL1 (Table 3). CHRDL1 is known to be a secreted antagonist of BMP4 activity (reviewed by Bragdon et al., 2011).

Regarding Notch signalling, the observed enrichment of JAG1 expression in the 3/4PP endoderm confirms previous data from our lab (Figueiredo et al., 2016), suggesting an endogenous paracrine effect regulating 3/4PP specification, possibly via NOTCH1, whose expression is enriched in PP endoderm, when comparing with anterior Pharynx endoderm (Figure 12).

Considering the number of genes found to be annotated to different signalling pathways, we find that the highest number in the 3/4PA mesenchyme is associated to the VEGF pathway followed by the Retinoic acid, BMP and Wnt pathways (in decreasing order).

In contrast, Wnt signalling seems to be the main up-regulated signalling pathway in 2PAd mesenchyme, suggesting its involvement in the inhibitory properties of this tissue (Figure 19a). The exception is WNT5A, which shows much higher expression in 3/4PA mesenchyme. In a comparable developmental process, it was shown that WNT5A secretion by dermal cells leads to autocrine FGF7 expression and consequent induction of FOXN1 expression in hair follicular cells (Hu et al., 2010). Our data also reveals FGF7 as the most enriched FGF-related transcript in 3/4PA mesenchyme, pointing to a similar WNT5A/FGF7/FOXN1 cascade in thymus induction at 3/4PP endoderm, probably mediated by fibroblast growth factor receptor R2-IIIb (Revest et al., 2001).

When comparing the heatmap of transcription profiles from 3/4PA mesenchyme with the 2PAd mesenchyme (Figure 17b), it became apparent their possible opposing roles. Examples of this dichotomy are INHBA, found upregulated in 3/4PA; and FST, upregulated in 2PAd.

INHBA encodes a subunit of Activin A, mainly expressed by pericytes (Bautista et al., 2021; Lepletier et al., 2019) and it was recently shown to be relevant for TEC differentiation (Lepletier et al., 2019). Conversely, FST (Follistatin) is an activin A antagonist and it was described to inhibit TEC differentiation (Lepletier et al., 2019). FST is mostly expressed by adult mesenchyme cells and subset of epithelial cells (Bautista et al., 2021).

	3/4PA mesenchyme		2PAd mesenchyme	
Signalling by VEGF (R-HSA-194138)	VEGFA	Vascular endothelial growth factor A	VEGFD	Vascular endothelial growth factor D
	KDR	Vascular endothelial growth factor receptor 2		
	PAK1	Serine/threonine-protein kinase PAK 1		
	CYFIP2	Cytoplasmic FMR1-interacting protein 2		
	HSPB1	Heat shock protein beta-1		
	MAPK11	Mitogen-activated protein kinase 11		
	MAPK12	Mitogen-activated protein kinase 12		
Signalling by Retinoic Ac. (R-HSA-5362517)	RARA	Retinoic acid receptor alpha	CYP26C1	Cytochrome P450 26C1
	CRABP1	Cellular retinoic acid-binding protein 1		
	ALDH1A2	Retinal dehydrogenase 2		
	DHRS3	Short-chain dehydrogenase/reductase 3		
	RDH10	Retinol dehydrogenase 10		
	CYP26A1	Cytochrome P450 26A1		
BMP signalling pathway (GO:0030509)	BMP2	Bone morphogenetic protein 2	CHRDL1	Chordin-like protein 1
	BMP4	Bone morphogenetic protein 4		
	BMP6	Bone morphogenetic protein 6		
	BMP7	Bone morphogenetic protein 7		
	BMP10	Bone morphogenetic protein 10		
	GDF6	Growth/differentiation factor 6		
Wnt signalling pathway (GO:0016055)	WNT2	Protein Wnt-2	WIF1	Wnt inhibitory factor 1
	WNT2B	Protein Wnt-2b	SFRP1	Secreted frizzled-related protein 1
	WNT5A	Protein Wnt-5a	APCDD1	Protein APCDD1
	FZD8	Frizzled-8	AXIN2	Axin-2
	SFRP2	Secreted frizzled-related protein 2	DAB2	Disabled homolog 2
	DKK3	Dickkopf-related protein 3	NKD1	Protein naked cuticle homolog 1
	CTNND2	Catenin delta-2	TLE1	Transducin-like enhancer protein 1
			LGR4	Leucine-rich repeat-containing G-protein coupled receptor 4
			DIXDC1	Dixin
			CPZ	Carboxypeptidase Z
			LEF1	Lymphoid enhancer-binding factor 1
Notch signalling pathway (GO:0007219)	HES5	Transcription factor HES-5	SNAI2	Zinc finger protein SNAI2
	HOXD3	Homeobox protein Hox-D3		
	NEURL1B	E3 ubiquitin-protein ligase NEURL1B		
Ephrin signalling (R-HSA-3928664)	EPHA4	Ephrin type-A receptor 4	EFNB1	Ephrin-B1
	PAK1	Serine/threonine-protein kinase PAK 1		
Signalling by FGFR (R-HSA-190236)	FGF7	Fibroblast growth factor 7	FGF19	Fibroblast growth factor 19
	FGFRL1	Fibroblast growth factor receptor-like 1	FLRT3	Leucine-rich repeat transmembrane protein FLRT3
	SPRY2	Protein sprouty homolog 2		
Hedgehog Signalling Pathway (WP4249)	-		-	

Table 3. Genes of main signalling pathways differentially expressed in PA mesenchyme. PA, Pharyngeal Arch.

To search for other signals that may regulate epithelial-mesenchymal interactions during PP endoderm specification, we performed a similar approach exploring gene enrichment for distinct signalling pathways by comparing the 3/4PP and 2PP endoderm (Figure 19b, and Table 4).

Notably, the most represented signalling pathways in 3/4PP and 2PP endoderm (Figure 19b) almost mirror the 3/4PA and 2PAd mesenchyme pathway profiles (Figure 19a). Again, transcripts for Wnt signalling components are enriched in 2PP endoderm, in comparison to 3/4PP endoderm. Together, these results reinforce the hypothesis of the Wnt pathway acting as a silencer at this developmental stage, similar to what is observed in later stages of thymus formation (Swann et al., 2017). As detailed above, a strong correlation was established between up-regulated genes in 2PP endoderm and GO-terms of negative regulation of developmental processes (Figure 14c).

In contrast, VEGF and Retinoic Acid pathways show the highest transcript enrichment in 3/4PP and 3/4PA tissues, suggesting an essential role of these pathways during epithelial-mesenchymal interactions to promote thymus formation. Retinoic acid is a diffusible mesodermal signal, described to positively regulate expression of factors like FGF8, PAX1, PAX9, early markers of PP endoderm; and Tbx1 and Hoxa3, involved in PP formation (Figueiredo et al., 2020; Quinlan et al., 2002). The up-regulation of transcripts for RARB and other RA pathway components (Table 3), accompanied by strong up-regulation of HOX-gene expression (Figure 14b and Figure 15) in 3/4PP endoderm, clearly point to a critical role of the RA/Hox gene pathway in establishing the identity of this pharyngeal pouch.

A closer examination of secreted VEGF ligands shows a differential enrichment of VEGFA and VEGFD transcripts in the 3/4PP-3/4PA and 2PP-2PAd environments, respectively (Figure 19). This finding suggests a distinct activation of VEGF pathway to either promote or repress thymus formation. In agreement, VEGFA deletion from thymic epithelial cells disrupts organ blood vessel architecture (Mü et al., 2005).

Finally, specific ligand-receptor interactions of Ephrin signalling are suggested when analysing Ephrin related transcripts that are differentially expressed in 3/4PA – 3/4PP and 2PAd – 2PP environments (Tables 3 and 4). Ephrin signalling is known to participate in several thymus developmental scenarios, including epithelium-mesenchyme interactions that determine epithelial cell polarity, positioning and proliferation (reviewed by Muñoz et al., 2011). EFNB2 null mice showed thymic defects, due to abnormal TECs morphology and differentiation, with consequent perturbation of thymocyte-TEC interactions (Cejalvo et al., 2015). EFNB2 ligand was shown to be required for thymus migration during organogenesis (K. E. Foster et al., 2010). Herein, we identify transcript enrichment for EPHB1 in 3/4PP endoderm, suggesting Ephrin signalling activation by this receptor during 3/4PP endoderm specification.

	3/4PP endoderm		2PP endoderm	
Signalling by VEGF (R-HSA-194138)	VEGFA	Vascular endothelial growth factor A	VEGFD	Vascular endothelial growth factor D
	NRP1	Neuropilin-1	PIK3R1	Phosphatidylinositol 3-kinase regulatory subunit alpha
	PIK3CB	Phosphatidylinositol 4,5-bisphosphate 3-kinase catalytic subunit beta isoform		
	PTK2	Focal adhesion kinase 1		
Signalling by Retinoic Ac. (R-HSA-5362517)	RARB	Retinoic acid receptor beta		
	CRABP1	Cellular retinoic acid-binding protein 1		
	RDH10	Retinol dehydrogenase 10		
BMP signalling pathway (GO:0030509)	CHRDL1	Chordin-like protein 1	GREM2	Gremlin-2
			GDF6	Growth/differentiation factor 6
			SOSTDC1	Sclerostin domain-containing protein 1
			TGFBR3	Transforming growth factor beta receptor type 3
Wnt signalling pathway (GO:0016055)			WNT2B	Protein Wnt-2b
			WNT3A	Protein Wnt-3a
			WNT6	Protein Wnt-6
			WNT7B	Protein Wnt-7b
			WNT7A	Protein Wnt-7a
			WNT9B	Protein Wnt-9b
			FZD10	Frizzled-10
			WIF1	Wnt inhibitory factor 1
			AXIN2	Axin-2
			APCDD1	Protein APCDD1
			DAB2	Disabled homolog 2
			LEF1	Lymphoid enhancer-binding factor 1
			RNF43	E3 ubiquitin-protein ligase RNF43
			KREMEN1	Kremen protein 1
			TRABD2A	Metalloprotease TIKI1
			NXN	Nucleoredoxin
			ROR1	Inactive tyrosine-protein kinase transmembrane receptor ROR1
			TLE1	Transducin-like enhancer protein 1
Notch signalling pathway (GO:0007219)	JAG1	Protein jagged-1	TP63	Tumor protein 63
	HEYL	Hairy/enhancer-of-split related with YRPW motif-like protein	SNAI2	Zinc finger protein SNAI2
			KAT2B	Histone acetyltransferase KAT2B
Ephrin signalling (R-HSA-3928664)	EPHB1	Ephrin type-B receptor 1	EFNB2	Ephrin-B2
	DNM1	Dynamin-1	EPHA1	Ephrin type-A receptor 1
	PTK2	Focal adhesion kinase 1	NGEF	Ephexin-1
			KALRN	Kalirin
Signalling by FGFR (R-HSA-190236)			ANOS1	Anosmin-1
			PIK3R1	Phosphatidylinositol 3-kinase regulatory subunit alpha
Hedgehog Signalling Pathway (WP4249)			SHH	Sonic hedgehog protein
			PTCH1	Protein patched homolog 1
			PTCH2	Protein patched homolog 2
			HHIP	Hedgehog-interacting protein
			LRP2	Low-density lipoprotein receptor-related protein 2

Table 4. Genes of main signalling pathways differentially expressed in PP endoderm. PP, Pharyngeal Pouch.

5

CONCLUSION

This project intended to enlighten the PP endoderm capacity to originate thymus and how this potential may be controlled by the microenvironment, the mesenchyme of the PA. Ultimately, we aimed to identify the conserved genetic program (s) that control thymic potential and to bring to light the molecular cues that render the mesenchyme-endoderm communication and interaction.

Our results showed that non-canonical pharyngeal pouches are able to generate morphological and functional thymus when interacting with permissive mesenchyme. This indicates a conserved program embodied in the endoderm of different PP, independent of their specific anatomic location. The transcriptomic analysis revealed a previously unnoticed Hox-code in the endoderm of the prospective thymus rudiment, besides the already well-characterized participation of HOXA2 and HOXA3. This high enrichment of Hox genes combinations in 3/4PP suggests their contribution to pouches identity and thymus fate specification.

In parallel, regulatory properties to thymus formation were identified in distinct PA mesenchyme. The 3/4PA mesenchyme has permissive properties to thymus formation while the dorsal region of 2PA mesenchyme holds inhibitory properties to the organ formation. The transcriptomic analysis revealed a clear contrast between the activated signalling pathways in the two mesenchyme, stressing their opposite roles. The Wnt signalling pathway was the main signalling pathway activated in the latter, pointing to its may involvement in the inhibitory properties of this mesenchyme.

Interestingly, RA pathway upregulation in 3/4PA mesenchyme and 3/4PP endoderm, revealed a possible epithelium-mesenchyme molecular cross-talk occurring early in development. Additionally, along with an expressive Hox code, RA/Hox pathway denote their importance in PP identity.

This research provided new insights into the molecular/genetic circuits controlling endoderm commitment into thymic epithelium during the early epithelium-mesenchyme interactions. A better knowledge of early thymus organogenesis not only

enriches fundamental biology, as it may also open new avenues to ex vivo generation of thymic organoids. Ultimately, this knowledge may enable new medical strategies targeting deficient thymus or generating functional T lymphocytes *in vitro*.

6
REFERENCES

Abramson, J., & Anderson, G. (2017). Thymic epithelial cells. In *Annual Review of Immunology* (Vol. 35, pp. 85–118). Annual Reviews Inc. https://doi.org/10.1146/annurev-immunol-051116-052320

Ainsworth, S. J., Stanley, R. L., & Evans, D. J. R. (2010). Developmental stages of the Japanese quail. *Journal of Anatomy*, *216*(1). https://doi.org/10.1111/j.1469-7580.2009.01173.x

Amaral, A. J., Brito, F. F., Chobanyan, T., Yoshikawa, S., Yokokura, T., Van Vactor, D., & Gama-Carvalho, M. (2014). Quality assessment and control of tissue specific RNA-seq libraries of Drosophila transgenic RNAi models. *Frontiers in Genetics*, *5*. https://doi.org/10.3389/fgene.2014.00043

Anders, S., Pyl, P. T., & Huber, W. (2015). HTSeq--a Python framework to work with high-throughput sequencing data. *Bioinformatics*, *31*(2), 166–169. https://doi.org/10.1093/bioinformatics/btu638

Anderson, G., & Jenkinson, E. J. (2001). Lymphostromal interactions in thymic development and function. *Nature Reviews*, *1*(Immunology), 31–40. https://doi.org/10.1038/35095500

Bautista, J. L., Cramer, N. T., Miller, C. N., Chavez, J., Berrios, D. I., Byrnes, L. E., Germino, J., Ntranos, V., Sneddon, J. B., Burt, T. D., Gardner, J. M., Ye, C. J., Anderson, M. S., & Parent, A. v. (2021). Single-cell transcriptional profiling of human thymic stroma uncovers novel cellular heterogeneity in the thymic medulla. *Nature Communications*, *12*(1). https://doi.org/10.1038/s41467-021-21346-6

Blackburn, C. C., Augustine, C. L., Li, R., Harvey, R. P., Malint, M. A., Boydt, R. L., Miller, J. F. A. P., & Morahan, G. (1996). The nu gene acts cell-autonomously and is required for differentiation of thymic epithelial progenitors (nude mice/thymus). In *Immunology* (Vol. 93).

Bleul, C. C., & Boehm, T. (2005). BMP signaling is required for normal thymus development. *Journal of Immunology (Baltimore, Md. : 1950)*, *175*(8), 5213–5221. https://doi.org/10.4049/jimmunol.175.8.5213

Bleul, C. C., Corbeaux, T., Reuter, A., Fisch, P., Mönting, J. S., & Boehm, T. (2006). Formation of a functional thymus initiated by a postnatal epithelial progenitor cell. *Nature*, *441*(7096), 992–996. https://doi.org/10.1038/nature04850

Bragdon, B., Moseychuk, O., Saldanha, S., King, D., Julian, J., & Nohe, A. (2011). Bone Morphogenetic Proteins: A critical review. In *Cellular Signalling* (Vol. 23, Issue 4, pp. 609–620). https://doi.org/10.1016/j.cellsig.2010.10.003

Bult, C. J., Blake, J. A., Smith, C. L., Kadin, J. A., Richardson, J. E., Anagnostopoulos, A., Asabor, R., Baldarelli, R. M., Beal, J. S., Bello, S. M., Blodgett, O., Butler, N. E., Christie, K. R., Corbani, L. E., Creelman, J., Dolan, M. E., Drabkin, H. J., Giannatto, S. L., Hale, P., … Zhu, Y. (2019). Mouse Genome Database (MGD) 2019. *Nucleic Acids Research*, *47*(D1), D801–D806. https://doi.org/10.1093/nar/gky1056

Calmont, A., Ivins, S., van Bueren, K. L., Papangeli, I., Kyriakopoulou, V., Andrews, W. D., Martin, J. F., Moon, A. M., Illingworth, E. A., Basson, M. A., & Scambler, P. J. (2009). Tbx1 controls cardiac neural crest cell migration during arch artery development by regulating Gbx2 expression in thepharyngeal ectoderm. *Development*, *136*(18), 3173–3183. https://doi.org/10.1242/dev.028902

Cejalvo, T., Munoz, J. J., Tobajas, E., Alfaro, D., García-Ceca, J., & Zapata, A. (2015). Conditioned deletion of ephrinB1 and/or ephrinB2 in either thymocytes or thymic epithelial cells alters the organization of thymic medulla and favors the appearance of thymic epithelial cysts. *Histochemistry and Cell Biology*, *143*(5), 517–529. https://doi.org/10.1007/s00418-014-1296-9

Chojnowski, J. L., Masuda, K., Trau, H. A., Thomas, K., Capecchi, M., & Manley, N. R. (2014). Multiple roles for HOXA3 in regulating thymus and parathyroid differentiation and morphogenesis in mouse. *Development (Cambridge)*, *141*(19), 3697–3708. https://doi.org/10.1242/dev.110833

Darnell, D. K., Kaur, S., Stanislaw, S., Davey, S., Konieczka, J. H., Yatskievych, T. A., & Antin, P. B. (2007). GEISHA: An in situ hybridization gene expression resource for the chicken embryo. *Cytogenetic and Genome Research*, *117*(1–4), 30–35. https://doi.org/10.1159/000103162

Dobin, A., Davis, C. A., Schlesinger, F., Drenkow, J., Zaleski, C., Jha, S., Batut, P., Chaisson, M., & Gingeras, T. R. (2013). STAR: ultrafast universal RNA-seq aligner. *Bioinformatics*, *29*(1), 15–21. https://doi.org/10.1093/bioinformatics/bts635

Duah, M., Li, L., Shen, J., Lan, Q., Pan, B., & Xu, K. (2021). Thymus Degeneration and Regeneration. In *Frontiers in Immunology* (Vol. 12). Frontiers Media S.A. https://doi.org/10.3389/fimmu.2021.706244

Enkhmandakh, B., & Bayarsaihan, D. (2015). Genome-wide Chromatin Mapping Defines AP2α in the Etiology of Craniofacial Disorders. *The Cleft Palate-Craniofacial Journal*, *52*(2), 135–142. https://doi.org/10.1597/13-151

Farley, A. M., Morris, L. X., Vroegindeweij, E., Depreter, M. L. G., Vaidya, H., Stenhouse, F. H., Tomlinson, S. R., Anderson, R. A., Cupedo, T., Cornelissen, J. J., & Clare, B. C. (2013). Dynamics of thymus organogenesis and colonization in early human development. *Development (Cambridge)*, *140*(9), 2015–2026. https://doi.org/10.1242/dev.087320

Figueiredo, M., & Neves, H. (2018). Two-step Approach to Explore Early-and Late-stages of Organ Formation in the Avian Model: The Thymus and Parathyroid Glands Organogenesis Paradigm Video Link. *J. Vis. Exp*, *5711437915*(13610). https://doi.org/10.3791/57114

Figueiredo, M., & Neves, H. (2019). Isolation of Embryonic Tissues and Formation of Quail-Chicken Chimeric Organs Using The Thymus Example. *Journal of Visualized Experiments*, *144*, e58965. https://doi.org/10.3791/58965

Figueiredo, M., Silva, J. C., Santos, A. S., Proa, V., Alcobia, I., Zilhão, R., Cidadão, A., & Neves, H. (2016). Notch and Hedgehog in the thymus/parathyroid common primordium: Crosstalk in organ formation. *Developmental Biology*, *418*(2), 268–282. https://doi.org/10.1016/j.ydbio.2016.08.012

Figueiredo, M., Zilhão, R., & Neves, H. (2020). Thymus inception: Molecular network in the early stages of thymus organogenesis. In *International Journal of Molecular Sciences* (Vol. 21, Issue 16, pp. 1–20). MDPI AG. https://doi.org/10.3390/ijms21165765

Flanagan, S. P. (1966). "Nude", a new hairless gene with pleiotropic effects in the mouse. In *Genet. Res., Camb (Vol. 8).* https://doi.org/10.1017/s0016672300010168

Foster, K. E., Gordon, J., Cardenas, K., Veiga-Fernandes, H., Makinen, T., Grigorieva, E., Wilkinson, D. G., Clare Blackburng, C., Richie, E., Manley, N. R., Adams, R. H., Kioussis, D., & Coles, M. C. (2010). EphB-ephrin-B2 interactions are required for thymus migration during organogenesis. *Proceedings of the National Academy of Sciences of the United States of America*, *107*(30), 13414–13419. https://doi.org/10.1073/pnas.1003747107

Foster, K., Sheridan, J., Veiga-Fernandes, H., Roderick, K., Pachnis, V., Adams, R., Blackburn, C., Kioussis, D., & Coles, M. (2008). Contribution of Neural Crest-Derived Cells in the

Embryonic and Adult Thymus 1. In *The Journal of Immunology* (Vol. 180). https://doi.org/10.4049/jimmunol.180.5.3183

Garcia, P., Wang, Y., Viallet, J., & Macek Jilkova, Z. (2021). The Chicken Embryo Model: A Novel and Relevant Model for Immune-Based Studies. In *Frontiers in Immunology* (Vol. 12). Frontiers Media S.A. https://doi.org/10.3389/fimmu.2021.791081

Gordon, J. (2018). Hox genes in the pharyngeal region: How hoxa3 controls early embryonic development of the pharyngeal organs. *International Journal of Developmental Biology*, *62*(11–12), 775–783. https://doi.org/10.1387/ijdb.180284jg

Gordon, J., A, B, Patel, S. R., Mishina, Y., & Manley, N. R. (2010). Evidence for an early role for BMP4 signaling in thymus and parathyroid morphogenesis. *Developmental Biology*, *339*(1), 141–154. https://doi.org/10.1016/j.ydbio.2009.12.026.Evidence

Gordon, J., Bennett, A. R., Blackburn, C. C., & Manley, N. R. (2001). Gcm2 and Foxn1 mark early parathyroid- and thymus-specific domains in the developing third pharyngeal pouch. *Mechanisms of development*, *103*(1-2), 141–143. https://doi.org/10.1016/s0925-4773(01)00333-1

Gordon, J., & Manley, N. R. (2011). Mechanisms of thymus organogenesis and morphogenesis. In *Development* (Vol. 138, Issue 18, pp. 3865–3878). https://doi.org/10.1242/dev.059998

Gordon, J., Wilson, V. A., Blair, N. F., Sheridan, J., Farley, A., Wilson, L., Manley, N. R., & Blackburn, C. C. (2004). Functional evidence for a single endodermal origin for the thymic epithelium. *Nature Immunology*, *5*(5), 546–553. https://doi.org/10.1038/ni1064

Hamazaki, Y. (2015). Adult thymic epithelial cell (TEC) progenitors and TEC stem cells: Models and mechanisms for TEC development and maintenance. In *European Journal of Immunology* (Vol. 45, Issue 11, pp. 2985–2993). Wiley-VCH Verlag. https://doi.org/10.1002/eji.201545844

Hamburger, V., & Hamilton, H. L. (1992). A series of normal stages in the development of the chick embryo. 1951. *Developmental dynamics : an official publication of the American Association of Anatomists*, *195*(4), 231–272. https://doi.org/10.1002/aja.1001950404

Hetzer-Egger, C., Schorpp, M., Haas-Assenbaum, A., Balling, R., Peters, H., & Boehm, T. (2002). Thymopoiesis requires Pax9 function in thymic epithelial cells. *European journal of immunology*, *32*(4), 1175–1181. https://doi.org/10.1002/1521-4141(200204)32:4<1175::AID-IMMU1175>3.0.CO;2-U

Hu, B., Lefort, K., Qiu, W., Nguyen, B. C., Rajaram, R. D., Castillo, E., He, F., Chen, Y., Angel, P., Brisken, C., & Dotto, G. P. (2010). Control of hair follicle cell fate by underlying mesenchyme through a CSL-Wnt5a-FoxN1 regulatory axis. *Genes and Development*, *24*(14), 1519–1532. https://doi.org/10.1101/gad.1886910

Ivins, S., van Beuren, K. L., Roberts, C., James, C., Lindsay, E., Baldini, A., Ataliotis, P., & Scambler, P. J. (2005). Microarray analysis detects differentially expressed genes in the pharyngeal region of mice lacking Tbx1. *Developmental Biology*, *285*(2), 554–569. https://doi.org/10.1016/j.ydbio.2005.06.026

Jerome, L. A., & Papaioannou, V. E. (2001). DiGeorge syndrome phenotype in mice mutant for the T-box gene, Tbx1 *Nature genetics*, *27*(3), 286–291. https://doi.org/10.1038/85845

Kamitani-Kawamoto, A., Hamada, M., Moriguchi, T., Miyai, M., Saji, F., Hatamura, I., Nishikawa, K., Takayanagi, H., Hitoshi, S., Ikenaka, K., Hosoya, T., Hotta, Y., Takahashi, S., & Kataoka, K. (2011). MafB interacts with Gcm2 and regulates parathyroid hormone expression and parathyroid development. *Journal of Bone and Mineral Research*, *26*(10), 2463–2472. https://doi.org/10.1002/jbmr.458

Khatri, S. B., & Groves, A. K. (2013). Expression of the Foxi2 and Foxi3 transcription factors during development of chicken sensory placodes and pharyngeal arches. *Gene Expression Patterns*, *13*(1–2), 38–42. https://doi.org/10.1016/j.gep.2012.10.001

Klein, L., Kyewski, B., Allen, P. M., & Hogquist, K. A. (2014). Positive and negative selection of the T cell repertoire: What thymocytes see (and don't see). In *Nature Reviews Immunology* (Vol. 14, Issue 6, pp. 377–391). Nature Publishing Group. https://doi.org/10.1038/nri3667

Kuleshov, M. v., Jones, M. R., Rouillard, A. D., Fernandez, N. F., Duan, Q., Wang, Z., Koplev, S., Jenkins, S. L., Jagodnik, K. M., Lachmann, A., McDermott, M. G., Monteiro, C. D., Gundersen, G. W., & Maayan, A. (2016). Enrichr: a comprehensive gene set enrichment analysis web server 2016 update. *Nucleic Acids Research*, *44*(1), W90–W97. https://doi.org/10.1093/nar/gkw377

Law, C. W., Chen, Y., Shi, W., & Smyth, G. K. (2014). voom: precision weights unlock linear model analysis tools for RNA-seq read counts. *Genome Biology*, *15*(2), R29. https://doi.org/10.1186/gb-2014-15-2-r29

Le Douarin, N. M., & Jotereau, F. V. (1975). Tracing of cells of the avian thymus through embryonic life in interspecific chimeras. *The Journal of Experimental Medicine*, *142*(1), 17–40. https://doi.org/10.1084/jem.142.1.17

Le Lièvre, C. S., & Le Douarin, N. M. (1975). Mesenchymal derivatives of the neural crest: analysis of chimaeric quail and chick embryos. *Journal of Embryology and Experimental Morphology*, *34*(1), 125–154.

Lepletier, A., Hun, M. L., Hammett, M. v., Wong, K., Naeem, H., Hedger, M., Loveland, K., & Chidgey, A. P. (2019). Interplay between Follistatin, Activin A, and BMP4 Signaling Regulates Postnatal Thymic Epithelial Progenitor Cell Differentiation during Aging. *Cell Reports*, *27*(13), 3887-3901.e4. https://doi.org/10.1016/j.celrep.2019.05.045

Li, T., Wernersson, R., Hansen, R. B., Horn, H., Mercer, J., Slodkowicz, G., Workman, C. T., Rigina, O., Rapacki, K., Stærfeldt, H. H., Brunak, S., Jensen, T. S., & Lage, K. (2017). A scored human protein–protein interaction network to catalyze genomic interpretation. *Nature Methods*, *14*(1), 61–64. https://doi.org/10.1038/nmeth.4083

Li, X., Oghi, K. a, Zhang, J., Krones, A., Bush, K. T., Glass, C. K., Nigam, S. K., Aggarwal, A. K., Maas, R., Rose, D. W., & Rosenfeld, M. G. (2003b). Eya protein phosphatase activity regulates Six1-Dach-Eya transcriptional effects in mammalian organogenesis. *Nature*, *426*(6964), 247–254. https://doi.org/10.1038/nature02283

Liu, Z., Yu, S., & Manley, N. R. (2007). Gcm2 is required for the differentiation and survival of parathyroid precursor cells in the parathyroid/thymus primordia. *Developmental Biology*, *305*(1), 333–346. https://doi.org/10.1016/j.ydbio.2007.02.014

Magaletta, M. E., Lobo, M., Kernfeld, E. M., Aliee, H., Huey, J. D., Parsons, T. J., Theis, F. J., & Maehr, R. (2022). Integration of single-cell transcriptomes and chromatin landscapes reveals regulatory programs driving pharyngeal organ development. *Nature Communications*, *13*(1), 457. https://doi.org/10.1038/s41467-022-28067-4

Manley, N. R., Richie, E. R., Blackburn, C. C., Condie, B. G., & Sage, J. (2011). Structure and function of the thymic microenvironment. In *Frontiers in Bioscience (Landmark edition)*, *16*(7), 2461–2477. https://doi.org/10.2741/3866

Martin, M. (2011). Cutadapt removes adapter sequences from high-throughput sequencing reads. *EMBnet.Journal*, *17*(1), 10. https://doi.org/10.14806/ej.17.1.200

Mü, S. M., Terszowski, G., Blum, C., Haller, C., Anquez, V., Kuschert, S., Carmeliet, P., Augustin, H. G., & Rodewald, H.-R. (2005). Gene targeting of VEGF-A in thymus epithelium disrupts thymus blood vessel architecture. *Proceedings of the National Academy of Sciences of the United States of America*, *102*(30), 10587–10592. https://doi.org/10.1073/pnas.0502752102

Muñoz, J. J., Cejalvo, T., Alonso-Colmenar, L. M., Alfaro, D., Garcia-Ceca, J., & Zapata, A. (2011). Eph/ephrin-mediated interactions in the thymus. In *NeuroImmunoModulation* (Vol. 18, Issue 5, pp. 271–280). Neuroimmunomodulation. https://doi.org/10.1159/000329490

Nehls, M., Kyewski, B., Messerle, M., Waldschütz, R., Schüddekopf, K., Smith, A. J., & Boehm, T. (1996). Two genetically separable steps in the differentiation of thymic epithelium. *Science (New York, N.Y.)*, *272*(5263), 886–889. https://doi.org/10.1126/science.272.5263.886

Neves, H., Dupin, E., Parreira, L., & le Douarin, N. M. (2012). Modulation of Bmp4 signalling in the epithelial-mesenchymal interactions that take place in early thymus and parathyroid development in avian embryos. *Developmental Biology*, *361*(2), 208–219. https://doi.org/10.1016/j.ydbio.2011.10.022

Nguyen, P. D., Hollway, G. E., Sonntag, C., Miles, L. B., Hall, T. E., Berger, S., Fernandez, K. J., Gurevich, D. B., Cole, N. J., Alaei, S., Ramialison, M., Sutherland, R. L., Polo, J. M., Lieschke, G. J., & Currie, P. D. (2014). Haematopoietic stem cell induction by somite-derived endothelial cells controlled by meox1. *Nature*, *512*(7514), 314–318. https://doi.org/10.1038/nature13678

Nitta, T., & Takayanagi, H. (2021). Non-Epithelial Thymic Stromal Cells: Unsung Heroes in Thymus Organogenesis and T Cell Development. In *Frontiers in Immunology* (Vol. 11). Frontiers Media S.A. https://doi.org/10.3389/fimmu.2020.620894

Nowell, C. S., Farley, A. M., & Blackburn, C. C. (2007). Thymus organogenesis and development of the thymic stroma. *Methods in molecular biology (Clifton, N.J.)*, *380*, 125–162. https://doi.org/10.1007/978-1-59745-395-0_8

Ohnemus, S., Kanzler, B., Jerome-Majewska, L. A., Papaioannou, V. E., Boehm, T., & Mallo, M. (2002). Aortic arch and pharyngeal phenotype in the absence of BMP-dependent neural crest in the mouse. *Mechanisms of development*, *119*(2), 127–135. https://doi.org/10.1016/s0925-4773(02)00345-3

Park, J.-E., Botting, R. A., Domínguez Conde, C., Popescu, D.-M., Lavaert, M., Kunz, D. J., Goh, I., Stephenson, E., Ragazzini, R., Tuck, E., Wilbrey-Clark, A., Roberts, K., Kedlian, V. R., Ferdinand, J. R., He, X., Webb, S., Maunder, D., Vandamme, N., Mahbubani, K. T., … Teichmann, S. A. (2020). A cell atlas of human thymic development defines T cell repertoire formation. *Science*, *367*(6480). https://doi.org/10.1126/science.aay3224

Patel, S. R., Gordon, J., Mahbub, F., Blackburn, C. C., & Manley, N. R. (2006). Bmp4 and Noggin expression during early thymus and parathyroid organogenesis. *Gene Expression Patterns GEP*, *6*(8), 794–799. https://doi.org/10.1016/j.modgep.2006.01.011

Quinlan, R., Gale, E., Maden, M., & Graham, A. (2002). Deficits in the posterior pharyngeal endoderm in the absence of retinoids. *Developmental Dynamics*, *225*(1), 54–60. https://doi.org/10.1002/dvdy.10137

Reijntjes, S., Stricker, S., & Mankoo, B. S. (2007). A comparative analysis of Meox1 and Meox2 in the developing somites and limbs of the chick embryo. *International Journal of Developmental Biology*, *51*(8), 753–759. https://doi.org/10.1387/ijdb.072332sr

Reimand, J., Kull, M., Peterson, H., Hansen, J., & Vilo, J. (2007). G:Profiler-a web-based toolset for functional profiling of gene lists from large-scale experiments. *Nucleic Acids Research*, *35*(SUPPL.2). https://doi.org/10.1093/nar/gkm226

Revest, J. M., Suniara, R. K., Kerr, K., Owen, J. J., & Dickson, C. (2001). Development of the thymus requires signaling through the fibroblast growth factor receptor R2-IIIb. *Journal of Immunology (Baltimore, Md. : 1950)*, *167*(4), 1954–1961. https://doi.org/10.4049/jimmunol.167.4.1954

Reynolds, K., Kumari, P., Sepulveda Rincon, L., Gu, R., Ji, Y., Kumar, S., & Zhou, C. J. (2019). Wnt signaling in orofacial clefts: crosstalk, pathogenesis and models. *Disease Models & Mechanisms*, *12*(2). https://doi.org/10.1242/dmm.037051

Reynolds, K., Zhang, S., Sun, B., Garland, M. A., Ji, Y., & Zhou, C. J. (2020). Genetics and signaling mechanisms of orofacial clefts. *Birth Defects Research*, *112*(19), 1588–1634. https://doi.org/10.1002/bdr2.1754

Ritchie, M. E., Phipson, B., Wu, D., Hu, Y., Law, C. W., Shi, W., & Smyth, G. K. (2015). limma powers differential expression analyses for RNA-sequencing and microarray studies. *Nucleic Acids Research*, *43*(7), e47–e47. https://doi.org/10.1093/nar/gkv007

Rizzoti, K., & Lovell-Badge, R. (2007). SOX3 activity during pharyngeal segmentation is required for craniofacial morphogenesis. *Development*, *134*(19), 3437–3448. https://doi.org/10.1242/dev.007906

Rodewald, H. R. (2008). Thymus organogenesis. In *Annual Review of Immunology* (Vol. 26, pp. 355–388). https://doi.org/10.1146/annurev.immunol.26.021607.090408

Stothard, C. A., Mazzotta, S., Vyas, A., Schneider, J. E., Mohun, T. J., Henderson, D. J., Phillips, H. M., & Bamforth, S. D. (2020). Pax9 and Gbx2 interact in the pharyngeal endoderm to

control cardiovascular development. *Journal of Cardiovascular Development and Disease*, *7*(2). https://doi.org/10.3390/JCDD7020020

Su, D. ming, Ellis, S., Napier, A., Lee, K., & Manley, N. R. (2001). Hoxa3 and Pax1 regulate epithelial cell death and proliferation during thymus and parathyroid organogenesis. *Developmental Biology*, *236*(2), 316–329. https://doi.org/10.1006/dbio.2001.0342

Swann, J. B., Happe, C., & Boehm, T. (2017). Elevated levels of Wnt signaling disrupt thymus morphogenesis and function. *Scientific Reports*, *7*(1). https://doi.org/10.1038/s41598-017-00842-0

Vaidya, H. J., Briones Leon, A., & Blackburn, C. C. (2016). FOXN1 in thymus organogenesis and development. In *European Journal of Immunology* (Vol. 46, Issue 8, pp. 1826–1837). Wiley-VCH Verlag. https://doi.org/10.1002/eji.201545814

Vitelli, F., Morishima, M., Taddei, I., Lindsay, E. A., & Baldini, A. (2002). Tbx1 mutation causes multiple cardiovascular defects and disrupts neural crest and cranial nerve migratory pathways. *Human molecular genetics*, *11*(8), 915–922. https://doi.org/10.1093/hmg/11.8.915

Vroegindeweij, E., Crobach, S., Itoi, M., Satoh, R., Zuklys, S., Happe, C., Germeraad, W. T. V., Cornelissen, J. J., Cupedo, T., Holländer, G. A., Kawamoto, H., & van Ewijk, W. (2010). Thymic cysts originate from Foxn1 positive thymic medullary epithelium. *Molecular Immunology*, *47*(5), 1106–1113. https://doi.org/10.1016/j.molimm.2009.10.034

Wei, Q., & Condie, B. G. (2011). A focused in situ hybridization screen identifies candidate transcriptional regulators of thymic epithelial cell development and function. *PLoS ONE*, *6*(11). https://doi.org/10.1371/journal.pone.0026795

Xu, P.-X., Zheng, W., Laclef, C., Maire, P., Maas, R. L., Peters, H., & Xu, X. (2002). Eya1 is required for the morphogenesis of mammalian thymus, parathyroid and thyroid. In *Development 129*(13), 3033–3044. https://doi.org/10.1242/dev.129.13.3033

Zou, D., Silvius, D., Davenport, J., Grifone, R., Maire, P., & Xu, P. X. (2006). Patterning of the third pharyngeal pouch into thymus/parathyroid by Six and Eya1. *Developmental Biology*, *293*(2), 499–512. https://doi.org/10.1016/j.ydbio.2005.12.015